Atmospheric
Chemistry
and Physics
Discussions

Open Access

The analysis of size-segregated cloud condensation nuclei counter (CCNC) data and its implications for aerosol-cloud interactions

M. Paramonov, P. P. Aalto, A. Asmi, N. Prisle, V.-M. Kerminen, M. Kulmala, and T. Petäjä

Department of Physics, University of Helsinki, P.O. Box 64, 00014 Helsinki, Finland

Correspondence to: M. Paramonov (mikhail.paramonov@helsinki.fi)

Discussion Paper | Discussion Paper | Discussion Paper | Discussion Paper

ACPD

13, 9681–9731, 2013

The analysis of size-segregated CCNC data

M. Paramonov et al.

Title Page

Abstract	Introduction
Conclusions	References
Tables	Figures

|◄ | ►|

◄ | ►

Back | Close

Full Screen / Esc

Printer-friendly Version

Interactive Discussion

Abstract

Ambient aerosol, CCN and hygroscopic properties were measured with a size-segregated CCNC in a boreal environment of Southern Finland at the SMEAR II station. The instrumental setup operated at five levels of supersaturation S covering a range from 0.1 to 1 % and measured particles with a size range of 20–300 nm; a total of 29 non-consecutive months of data are presented. The median critical diameter D_c ranged from 150 nm at S of 0.1 % to 46 nm at S of 1.0 %. The median aerosol hygroscopicity parameter κ ranged from 0.41 at S of 0.1 % to 0.14 at S of 1.0 %, indicating that ambient aerosol in Hyytiälä is less hygroscopic than the global continental or European continental averages. It is, however, more hygroscopic than the ambient aerosol in an Amazon rainforest, a European high alpine site or a forested mountainous site. A fairly low hygroscopicity in Hyytiälä is likely a result of a large organic fraction present in the aerosol mass comparative to other locations within Europe. A considerable difference in particle hygroscopicity was found between particles smaller and larger than ~100 nm in diameter, possibly pointing out to the effect of cloud processing increasing κ of particles > 100 nm in diameter. The hygroscopicity of the smaller, ~50 nm particles did not change seasonally, whereas particles with a diameter of ~150 nm showed a decreased hygroscopicity in the summer, likely resulting from the increased VOC emissions of the surrounding boreal forest and secondary organic aerosol (SOA) formation. For the most part, no diurnal patterns of aerosol hygroscopic properties were found. Exceptions to this were the weak diurnal patterns of small, ~50 nm particles in the spring and summer, when a peak in hygroscopicity around noon was observed. No difference in CCN activation and hygroscopic properties was found on days with or without atmospheric new particle formation. During all seasons, except summer, a CCN-inactive fraction was found to be present, rendering the aerosol of 75–300 nm in diameter as internally mixed in the summer and not internally mixed for the rest of the year.

1 Introduction

Aerosol particles are omnipresent in the Earth's atmosphere and are known to have an impact on climate (e.g. McCormick and Ludwig, 1967; Twomey, 1974; Lohmann and Feichter, 2005), visibility (e.g. Jinhuan and Liquan, 2000; Seinfeld and Pandis, 2006) and human health (e.g. Seaton et al., 1995; Finlayson-Pitts and Pitts, 1997; Hinds, 1999). From a climate perspective, aerosol particles directly interfere with the incoming solar and outgoing terrestrial radiation, as well as influence the Earth's radiation balance through their interactions with clouds. Through a variety of microphysical processes atmospheric particles influence the albedo, lifetime and precipitation patterns of clouds in what is known as the indirect effects of aerosols on climate (Forster et al., 2007). As noted in the Fourth Assessment Report of the Intergovernmental Panel on Climate Change (IPCC), the quantification of these indirect effects presents a major uncertainty in the current modelling and understanding of the aerosol-climate interactions, signifying the inclusion of clouds in the triple aerosol-cloud-climate system.

The aerosol particles participating in cloud formation are commonly known as cloud condensation nuclei (CCN), and their relevant behaviour in the atmosphere is dictated by their CCN activation and hygroscopic properties, i.e. their ability and likelihood to attract and retain water vapour molecules by means of condensation. It is important to remember that the activation of an aerosol particle into a cloud drop depends on the multitude of processes and atmospheric conditions prevalent during the particle formation and lifetime (McFiggans et al., 2006; Reutter et al., 2009). Besides the particle properties themselves, such as the number concentration, size and chemical composition, whether a particle can act as a CCN also depends on the partial pressure of the water vapour in the atmosphere (Pruppacher and Klett, 1997).

Atmospheric CCN have been studied extensively, and a multitude of studies exists related to the activation of CCN into cloud drops. Atmospheric CCN concentrations and size-resolved activation spectra have been presented in numerous studies (e.g. Gras, 1990; Gunthe et al., 2009; Sihto et al., 2011). A number of CCN closure studies

has been conducted (e.g. VanReken et al., 2003; Broekhuizen et al., 2006; McFiggans et al., 2006; Rissman et al., 2006), and the effect of organics and aerosol mixing state on CCN has been investigated as well (e.g. Cruz and Pandis, 1997; Wang et al., 2008, 2010). From a theoretical perspective, the Köhler theory and droplet growth kinetics have also been examined (e.g. Kulmala et al., 1993; Asa-Awuku and Nenes, 2007; Engelhart et al., 2008; Prisle et al., 2010). Due to logistical matters and limitations, various in situ in-cloud measurements of CCN activation present a challenge, and have only been conducted at a small number of sites (e.g. Baltensperger et al., 1997; Hatakka et al., 2003; Leskinen et al., 2009; van Pinxteren et al., 2012). At the same time, surface measurements, while easier to implement and with many measurement options available, are mostly limited to short-term campaigns (e.g. Gunthe et al., 2009; Cerully et al., 2011). Therefore, there is most definitely a need for more comprehensive long-term measurements of CCN activation and hygroscopicity around the world in order to improve the understanding of aerosol-cloud interactions and the modelling of the future climate.

This paper presents a unique dataset of CCN activation and hygroscopic properties measured in the boreal environment of Southern Finland with a cloud condensation nuclei counter (CCNC). The measurement setup utilised in this study allowed both to estimate the particle size at which the aerosol in a boreal environment becomes important for cloud formation, as well as to infer its chemical composition. Since measurements were conducted at different supersaturation levels, relevant physical and chemical properties of CCN were determined for particles of different sizes. Aerosol mixing state was also indirectly determined, dividing the whole aerosol population into the CCN-active and CCN-inactive fractions. The uniqueness of the dataset stems from its duration – a total of 29 months of data are presented here, making it the longest dataset of ambient CCN activation and hygroscopic properties measured with a size-resolved CCNC. The aim of this paper is to describe the CCN activation of ambient aerosol in a boreal environment, both with respect to its size and chemistry in order to (i) investigate the presence of temporal (viz. diurnal and seasonal) variations of these

|◀ | ▶|

◀ | ▶

Back | Close

Full Screen / Esc

properties, (ii) to determine the aerosol mixing state and its seasonality, (iii) to compare the derived values and variations with previously published results, and, finally, (iv) to provide the comprehensive insight into aerosol-cloud interactions in the boreal environment with the outcomes possibly applicable to other boreal regions of the world.

2 Theory

In the atmosphere the formation of water droplets occurs as a result of condensation during the conditions of supersaturation S of air with respect to water vapour. While homogeneous nucleation of supersaturated water vapour is possible in laboratory conditions, the S required for this process to onset is on the order of several hundred percent and does not occur in the atmosphere (Andreae and Rosenfeld, 2008). Aerosol particles, always present in the atmosphere, act as seeds for cloud droplet formation at S levels much lower than those required for homogeneous nucleation, i.e. just a few percent. Therefore, the condensation of supersaturated water vapour onto the aerosol particles is the only significant pathway of cloud droplet formation in the atmosphere (Pruppacher and Klett, 1997). These aerosol particles are known as Cloud Condensation Nuclei (CCN). The number of CCN in any given air mass may vary by several orders of magnitude, depending on the origin, and the spatial and temporal variation of CCN concentrations around the globe has been highlighted in various previous studies (e.g. Twomey and Wojciechowski, 1969; Hobbs et al., 1980; Snider and Brenguier, 2000; Roberts et al., 2006).

From a thermodynamic point of view, the number of CCN is directly related to the ambient supersaturation within the air mass; Köhler theory indicates that higher S results in higher CCN concentration, in other words, as S increases, smaller particles can activate as cloud droplets (Köhler, 1936; Seinfeld and Pandis, 2006; Reutter et al., 2009). It is, therefore, important to remember that varying degrees of S will affect the aerosol of different properties, i.e. its size, hygroscopicity and the mixing state. However, the concept of CCN is not to be confused with the cloud droplet number concentration

(CDNC) – while the CCN concentration is not dependent on cloud dynamics, the CDNC depends strongly on both aerosol particle number concentration and supersaturation S, which, in turn, is affected by updraft velocities, aerosol number size distribution and its chemical composition (Leaitch et al., 1992; Snider et al., 2003). It is assumed in this paper that the growth of cloud droplets in warm stratiform clouds occurs on a very short time scale at a constant S, and, therefore, the effect of aerosol number size distribution on ambient S is not considered in this paper. Besides the total aerosol number concentration and ambient S, the ability of aerosol particles to act as CCN is strongly linked to their physical and chemical properties, such as aerosol critical diameter D_c and hygroscopicity parameter κ (Petters and Kreidenweis, 2007). A multitude of literature exists on the effects of physics and chemistry of aerosol particles on their ability to act as CCN (e.g. Roberts et al., 2002; Dusek et al., 2006; McFiggans et al., 2006); aerosol mixing state has also been investigated with respect to its influence on CCN properties (e.g. Cubison et al., 2008; Su et al., 2010; Ervens et al., 2010).

There exist several techniques and measurement setups aimed at measuring and describing the properties of CCN. Number concentration of CCN-sized aerosol can be indirectly estimated from any instrument measuring aerosol size distributions at relevant sizes, such as the Differential Mobility Particle Sizer (DMPS); however, defining a lower limit of particle diameter is important. Since ambient in-cloud levels of S may vary both spatially and temporally, several lower limits have been proposed, e.g. 50 nm (Roberts et al., 2002; Lihavainen et al., 2003), 80 nm (Komppula et al., 2005; Asmi et al., 2011b); Asmi et al. (2011a) and Kerminen et al. (2012) included several other lower limits in an attempt to cover a wide range of S encountered in various ambient environments. The direct measurement of ambient CCN concentrations requires a measurement setup where ambient particles are counted, subjected to a certain known S, and then counted again. For such measurements various chambers can be used, such as a thermal gradient diffusion cloud chamber (e.g. Covert et al., 1998), coupled with particle counters and, possibly, a Differential Mobility Analyser (DMA) in case the knowledge about a particular particle size is required. One such thermal gra-

dient diffusion chamber constitutes the main component of the CCNC, an instrument commonly used to measure ambient CCN concentrations and to derive various CCN properties (Roberts and Nenes, 2005). It has been used to measure both total (e.g. Sihto et. al., 2011) and size-resolved (e.g. Gunthe et al., 2009) CCN concentrations.

The critical diameter D_c is typically defined as the smallest particle size at which particles are activated and can grow to cloud droplet size under certain ambient conditions; this size is directly related to S through the Köhler theory (Pruppacher and Klett, 1997). While in theory this size separates particles into completely non-activated and activated fractions, in practice however, due to ambient aerosol commonly being externally mixed, it is typically defined as the size at which 50 % of particles grow to cloud droplets. Sihto et al. (2011) estimated both the activated fractions and D_c by comparing CCN number concentrations measured by the CCNC to the total number concentration (N_{CN}) measured by the DMPS. If size-segregated CCN measurements are available, such as when coupling CCNC with a DMA, D_c can be directly estimated from activation spectra, i.e. by plotting the N_{CCN}/N_{CN} ratios as a function of size and defining the point on a curve at which a certain fraction of aerosol particles activates (typically, 50 %) (e.g. Rose et al., 2008). Such measurement setup has been utilized in numerous studies (e.g. Corrigan and Novakov, 1999; Petters et al., 2007; Gunthe et al., 2009).

Coupling aerosol particle dry size and its chemical composition is imperative for understanding the aerosol-water interactions (McFiggans et al., 2006), and there exists a number of approaches aimed at describing them (e.g. Fitzgerald et al., 1982; Svenningsson et al., 1992; Rissler et al., 2005; Rissler et al., 2006; Khvorostyanov and Curry, 2007; Padró et al., 2007). The hygroscopicity parameter κ (Petters and Kreidenweis, 2007) is a unitless parameter describing the relationship between particle dry diameter, its chemical composition and the ambient S. For ambient atmospheric aerosol κ values fall within the range of $0.1 < \kappa < 0.9$, and owing to the simplicity of its computation, it has been widely used in numerous studies (e.g. Merikanto et al., 2009; Kammermann et al., 2010; Rose et al., 2010; Sihto et al., 2011). There are several

ways to determine κ using ambient measurements; these can be performed by various instruments under both subsaturated and supersaturated conditions. CCN activation spectra measured by the aforementioned CCNC can be used to determine κ by applying the effective hygroscopicity parameter (EH1) Köhler model (Rose et al., 2008). Critical diameters D_c calculated from activation spectra paired up with the known prescribed CCNC supersaturation level can be used in this model to determine κ utilising Eq. (1):

$$S = \frac{D_{\text{wet}}^3 - D_s^3}{D_{\text{wet}}^3 - D_s^3(1 - \kappa)} \exp\left(\frac{4\sigma_{\text{sol}}M_{\text{w}}}{RT\rho_{\text{w}}D_{\text{wet}}}\right), \tag{1}$$

where S is water vapour saturation ratio, D_{wet} is the droplet diameter, D_s is the dry particle diameter, κ is hygroscopicity parameter, σ_{sol} is the surface tension of condensing solution, M_{w} is the molar mass of water, R is the universal gas constant, T is the absolute temperature and ρ_{w} is the density of pure water. As per Rose et al. (2008), D_s can be substituted with D_c and σ_{sol} is taken that of pure water (0.072 J m^{-2}); T is recorded by the CCNC for each spectrum. κ values can be determined by varying κ and D_{wet} so that S is equal to the prescribed supersaturation inside the chamber S_{eff} and to the maximum of the Köhler model curve of CCN activation.

Hygroscopicity Tandem Differential Mobility Analyzer (H-TDMA) is another common measurement setup used to determine D_c, κ and other relevant CCN properties at subsaturated conditions (Ehn et al., 2007; Swietlicki et al., 2008). The growth factors measured by the H-TDMA can be used together with, e.g. the EH1 Köhler model equation to determine both D_c and κ. Since both CCNC and H-TDMA provide information about the hygroscopic growth of aerosol particles and other CCN properties, it has been common to run these measurements in parallel to conduct the so-called CCN closure studies, in which the results of the two instruments are evaluated and compared. The summary of such studies can be found in McFiggans et al. (2006).

As stated above, due to the simplicity of estimating the hygroscopicity parameter κ of ambient aerosol as described by Petters and Kreidenweis (2007), numerous studies,

based both on ambient measurements and model simulations, have reported κ values for various locations around the globe. Both Andreae and Rosenfeld (2008) and Pringle et al. (2010) studied the hygroscopicity of the aerosol on a global scale. Several measurement campaigns have also attempted to describe the hygroscopicity of European aerosol (e.g. Dusek et al., 2006; Kandler and Shütz, 2007; Bougiatioti et al., 2009). Gunthe et al. (2009), Jurányi et al. (2011) and Levin et al. (2012) all used a similar measurement setup to describe the hygroscopicity of aerosol in an Amazonian rainforest, high alpine site Jungfraujoch in Switzerland and a forested mountainous site in Colorado, respectively. There also exists a number of CCN hygroscopicity studies based on short-term measurement campaigns in the boreal environment, namely Hyytiälä Forestry Field Station, which is also the location of long-term CCN measurements presented in this paper (e.g. Sihto et al., 2011; Cerully et al., 2011). Temporal patterns of aerosol hygroscopic properties have also been reported in existing literature; however, due to the majority of studies being short-term measurement campaigns, mostly diurnal patterns of D_c and κ have been reported. Seasonal variation has been reported in a modelling study by Pringle et al. (2010) and in several experimental studies (Cerully et al., 2011; Jurányi et al., 2011; Sihto et al., 2011; Levin et al., 2012).

3 Methodology

3.1 Measurement site

CCNC measurements have been conducted at the SMEAR II (Station for Measuring Ecosystem-Atmosphere Relations) site in Hyytiälä Forestry Field Station, and they form a part of the comprehensive network of aerosol- and meteorology-related measurements in Southern Finland (Hari and Kulmala, 2005). The station (61° 50′ 50.685″ N, 24° 17′ 41.206″ E, 181 m a.m.s.l.) is located 220 km north-northwest of Helsinki on a flat terrain surrounded by a boreal coniferous forest, mainly Scots pine, and is, therefore, well representative of the boreal environment. The nearest city of Tampere (pop.

215 000) lies 50 km southwest; the station may, therefore, be described as a rural background site. SMEAR II is subject to both clean maritime air masses, as well as to more polluted (and less frequent) continental air masses; however, most often both of these air mass types are characterized by low aerosol particle number concentrations (Sogacheva et al., 2005).

3.2 Instrumentation

The setup for size-resolved CCN measurements is a multi-component system, consisting of the Differential Mobility Analyzer (DMA), Condensation Particle Counter (CPC) and the CCNC unit itself, which includes a saturator column and an Optical Particle Counter (OPC). The CCNC is a commercially available instrument, distributed by the Droplet Measurement Technologies (DMT), Inc., and its main component is a continuous-flow streamwise thermal-gradient diffusion chamber. At SMEAR II the CCNC model is DMT CCN-100, and it has been operating continuously since July 2008. A more detailed discussion, than what follows below, about the operating principles of the DMT-CCNC, can be found in Roberts and Nenes (2005) and in Rose et al. (2008).

As the aerosol is entering the measurement setup through an inlet mounted approximately 8 m above the ground, it is first dried with a Nafion drier, following which the particles are neutralised with a 370 MBq ^{13}C radioactive source in order to achieve an equilibrium charge distribution. Afterwards the dry aerosol with a known charge distribution enters the DMA system, which categorizes the particles according to their physical dimensions based on the principle of the aerosol electrical mobility (Aalto, 2004). The specific DMA in question is a Hauke-type DMA with a concentric cylindrical configuration and a length of 28 cm. The DMA is a key component for size-segregated CCNC measurements, and it sorts the particles into 30 logarithmically distributed size bins, with size ranging from 20 to 300 nm. Following this, the flow of the monodisperse aerosol of a known size is split into two parallel lines, with the first leading to the laminar flow type CPC (model TSI 3772; sample flow 1 ± 0.015 L min^{-1}; sheath flow 14 L min^{-1}),

which determines the total particle number concentration of that particular size. This quantity is hereafter referred to as N_{CN}. The second parallel line leads to the CCNC unit itself. At the SMEAR II the CCNC saturator unit is a vertical flow tube of cylindrical shape with an inner diameter of 2.3 cm and a length of 50 cm. Inside this chamber the aerosol flows from the top to bottom with a flow rate of $0.45 \pm 0.02 \, L \, min^{-1}$, surrounded by the filtered sheath air with a sheath-to-aerosol flow ratio of 10; aerosol flow occurs under laminar conditions and near-ambient pressure. The thermal electric coolers (TEC) and thermocouples mounted at the beginning, middle and end of the outer tube wall create and monitor a near-linear positive temperature gradient within the tube. The inner walls of the flow tube are continuously wetted with liquid water. During the passage of the laminar flow through the tube, heat and water vapour are effectively transported from the inner walls to the centerline of the tube, thus creating a constant uniform water vapour supersaturation S_{eff} along the centerline. The CCNC in question operates at five levels of S_{eff}: 0.1, 0.2, 0.4, 0.6 and 1.0 %. As the monodisperse aerosol flows through the tube, those particles with smaller critical supersaturation S_{c} than S_{eff} will grow by the condensation of water vapour, i.e. activate as CCN. The typical residence time of the aerosol particles in the saturator unit is on the order of 10 s – sufficient enough for particles to grow to ∼ 1 µm in diameter. The activated particles are then counted by the OPC, and this quantity is hereafter referred to as N_{CCN}. In order to assure the quality of the CCNC data, the CCNC is calibrated approximately every two months using nebulised, dried, charge-equilibrated and size-segregated ammonium sulphate aerosol, and the procedure is carried out as per Rose et al. (2008). These calibrations reveal a consistent overestimation of presumed S_{eff} of 0.1 % by up to 10 % and the underestimation of presumed S_{eff} of 0.2 and 0.4 % by up to 12 and 7 %, respectively.

For a given S_{eff} both prior to and after the measurement of each activation spectrum, the instrument also measures the total, non-size-segregated concentration of both N_{CN} and N_{CCN}, (DMA bypassed). The non-size-segregated CCNC measurements are not discussed in this paper. The full scan at one S_{eff} takes, on average, 17 min 40 s, with

activation spectrum taking 17 min. Prior to 25 January 2010, between 13 and 40 s were allocated for the saturator unit to adjust to a new, higher S_{eff}; 3 min 20 s were allocated for adjusting from the S_{eff} of 1.0 to 0.1 %. From 25 January 2010 onwards these times have been increased to 1 min 10 s and 15 min for an upward and a downward shift in S_{eff}, respectively. Therefore, slightly more than three full activation spectra per hour were measured by the instrument prior to 25 January 2010, and slightly less than three full activation spectra per hour after that date. The statistics about data coverage presented in the next section are based on these numbers.

3.3 Data description

This paper presents the analysis of size-segregated CCNC data from SMEAR II from 10 February 2009 until 30 April 2012. Despite continuous measurements, from 9 July 2010 until 9 May 2011 the instrument was operating at levels of S_{eff} different from those indicated above. This occurred due to a miscalibration of the instrument, and the data from this period are not included in the analysis. The dataset has undergone a rigorous procedure of cleaning and processing in order to remove bad data – due to the complexity of the measurement setup and absence of standardized procedures for working with size-segregated CCNC data, this was the most challenging and time consuming part of the analysis. Figure 1 presents the data availability for the whole measurement period. The results presented below are based on a total of 46 400 activation spectra.

For each spectrum the activated fraction A was calculated for each size bin by dividing N_{CCN} by the corresponding N_{CN}. The following cumulative Gaussian (normal) distribution function based on the non-linear least-squares fitting method was then fitted to each activation spectrum:

$$A = a \left(1 + \mathrm{erf} \left(\frac{D - D_a}{\sigma \sqrt{2}} \right) \right), \tag{2}$$

where a is half the maximum value of A in each spectrum, erf is the error function, D is the fitted particle diameter, D_a is the particle diameter at $A = a$, and σ is the stan-

dard deviation of the cumulative Gaussian distribution function, as described in Rose et al. (2008). In the function above the parameter D_a is the critical diameter of dry aerosol particles D_c, which in this study is defined as the diameter at which half of the incoming particles are activated at a certain S_{eff}. Two methods were used to fit Eq. (2)

5   to each activation spectrum. The first method closely follows that proposed by Rose et al. (2008), in which all A in each activation spectrum are normalized to unity, i.e. divided by the maximum A. In this method D_a and σ are the fit parameters, where D_a is the critical diameter D_c at $a = 0.5$, and the maximum activated fraction (MAF) is 1 (Fig. 2, left panel). Hereafter, this method is referred to as normalised.

10   Since the measurements deal with ambient aerosol, which can be externally mixed, and since a significant variation was observed in A at larger sizes, a second fitting method was used, where no normalisation of A was carried out and a was the third fit parameter. In this method the function found the best fit to each spectrum regardless of where it levelled out at larger sizes (MAF and a are not specified and allowed to vary),

15   and D_c was found as D_a at a (Fig. 2, right panel). Hereafter, this method is referred to as non-normalised. As per Rose et al. (2010), the normalised method gives properties of the external mixture of both CCN-active and CCN-inactive aerosol, while the non-normalised method specifically considers only the CCN-active fraction of the aerosol population. The κ values were calculated using Eq. (1) using both sets of D_c derived

20   using normalised and non-normalised methods. It is important to note here that both fitting methods yielded physically unreasonable D_c and κ values for a small amount of data, and 0.4 % of all activation spectra were excluded from the analysis.

    The activation spectra were not corrected for effects of the DMA transfer function, as these effects are assumed to be negligible in the described measurement setup.

25   The effects of doubly charged particles were investigated for a subset of spectra at S_{eff} of 0.1 and 0.2 % by determining the fraction of activated doubly charged particles and assuming that this fraction is constant over the whole size range (Rose et al., 2008). In the majority of investigated cases this fraction of activated doubly charged particles was small (< 0.1), and it was found that correcting the spectra for the doubly charged

particles increases D_c by an average of 2 %, rendering the implementation of correction procedure for the whole dataset unnecessary.

4   Results and discussion

As mentioned previously, a total of 46 400 activation spectra were collected, processed and analysed in this study; this number was roughly equally distributed among the five levels of S_{eff}. The median values and variability of the total particle number and CCN concentrations, as well as of the activated fraction for two levels of S_{eff} are presented in Fig. 3. As expected, a larger number of particles activated at a higher S_{eff}; this is also signified by the s-shaped activation curve moving to the left in the right panel of the figure (i.e. smaller size). In the studied 20–300 nm size range, the highest concentrations were found in the upper end of the Aitken mode, around 80–100 nm. While the median concentrations in these size bins are approximately at 12 particles cm^{-3}, the percentiles indicate that a large variation in number concentrations is present.

Several things are of interest in Fig. 3. First, the largest size bin of 300 nm exhibited a fairly large variation of A values; the median A in this size bin at the S_{eff} of 1.0 % is above unity. This, while physically unreasonable, is a direct consequence of very low particle number concentrations at this size, and may also stem from different counting efficiencies of the CPC and the OPC. The 300 nm particle size bin was not excluded from the dataset due to its presumably low impact on the Eq. (2) fitting method, especially so for the non-normalised procedure. Second, the variability of A increased with an increase in particle size – this is also related to low particle number concentrations and counting statistics. Third, while certain activation spectra, especially at lower S_{eff}, did exhibit a secondary plateau of doubly charged particles, this plateau is not visible in the left side of Fig. 3, indicating its infrequent occurrence and further explaining the reasons behind the decision of not correcting the spectra for doubly charged particles. The results of the normalised and non-normalised fitting of Eq. (2), the related terms

and the derived parameters of D_c and κ are shown in Table 1; these are presented separately for each S_{eff}, as well as for the whole dataset.

4.1 Method comparison

While both normalised and non-normalised methods are intended to provide hygroscopic properties of an aerosol population, their differences in describing the respective entire aerosol population and only the CCN-active fraction of the population are clearly evident (Table 1). For each fitting of Eq. (2) to the activation spectrum, a root mean square error (RMSE) was calculated to estimate the appropriateness of the fit. While for the lowest S_{eff} of 0.1 % the median RMSE of Eq. (2) fit was the same for both methods, for all other S_{eff} the goodness of the fit was worse for the normalised method. This feature is a direct consequence of the inclusion of the presumably present CCN-inactive fraction in the fit of the normalised method, and the normalised method fit being largely dependent on one, maximum observed, A value in each spectrum.

For all levels of S_{eff}, both separately and overall, D_c values and their variation in the normalised method are both higher than those in the non-normalised method. In fact, 97.4 % of all D_c from normalised method are higher than the corresponding D_c from non-normalised method (Fig. 4). Logically, if one includes the CCN-inactive fraction in Eq. (2) fit, the overall hygroscopicity of the aerosol population in question would decrease, increasing the critical diameter needed for CCN activation. The remaining few percent visible in Fig. 4 above the black 1 : 1 line result from those spectra at S_{eff} of 0.1 % where the number of A points close to unity was very low and the resulting non-normalised Eq. (2) fit curve levelled out at values of MAF much higher than unity.

Following what has been stated above, κ values from the normalised method are generally lower than those from the non-normalised method (Table 1). The results of the comparison of methods presented above with respect to D_c and κ agree well with those reported by Gunthe et al. (2009). The non-normalised method, besides describing only the CCN-active fraction of the aerosol, also provides insight into the aerosol mixing state by way of quantifying the CCN-inactive fraction of the aerosol population,

a topic further examined in Sect. 4.6. In order to carefully describe the CCN activity of an ambient aerosol population, and taking into account the fact that the non-normalised method demonstrates the properties of CCN-active aerosol fraction and provides insight into the aerosol mixing state, from this point forward only the D_c and κ values
5 from non-normalised method are discussed, unless otherwise specified.

4.2 General patterns in data

It is clearly visible from Table 1 that the function fit, as shown by the RMSE, was best at S_{eff} of 0.1 % and worsened as S_{eff} increased. For the highest S_{eff} the modelled A deviated by up to 15 % from observed A as seen by the 75th percentile of the RMSE.
10 Having mentioned the decreasing absolute particle number concentrations at sizes larger than $\sim 100\,nm$ and the resulting poor statistics of A, this increase in RMSE is not surprising. It was observed that while the function modelled A very well for small, non-activated particles and during the slope of the s-shaped curve, the largest differences in the observed and modelled A were found where the function reached MAF (Fig. 2).
15 The increased RMSE at higher S_{eff} is not expected to greatly affect the derived D_c; it does, however, call for a strict mathematical definition of the observed MAF. With respect to the mid-point a of the modelled A spectrum and MAF, there is no significant correlation with S_{eff}. Both a and MAF are indicative of the CCN-active and -inactive fractions of the aerosol.
20 The median critical diameter D_c ranged from 150 nm at S of 0.1 % to 46 nm at S of 1.0 %. As expected from the Köhler theory, the median D_c decreases with increasing S_{eff}, and as expected from Eq. (1) this decrease is exponential (Fig. 5). From the lowest to highest S_{eff} the critical diameter D_c decreases by over a 100 nm from the lower end of accumulation mode to the mid-point of the Aitken mode. Considering that high-
25 est number concentrations within the 20–300 nm size range were found in the upper end of the Aitken mode, a change in ambient S has a strong impact on the number of particles that can act as CCN and, consequently, the number of cloud drops formed. When the quartiles of the median D_c are examined, it is obvious that the variation in

calculated D_c also diminishes with increasing S_{eff}. This may stem from the fact that in general at higher S_{eff} more particles activate, as well as that there are more A points close to MAF at the larger end of the size spectrum, improving both the fit and statistics, and reducing the uncertainty and variation. The exponential decrease of both median D_c and its variation with increasing S_{eff} indicates that a change in ambient S at smaller values (e.g. $0.05 < S < 0.3\%$) has a larger effect on the number of CCN than a change in ambient S at higher values (e.g. $0.5 < S < 1\%$). This notion is important to keep in mind considering that the typical levels of ambient S found in warm stratiform clouds in the boreal environment of the measurement site are typically low (Seinfeld and Pandis, 2006; Lihavainen et al., 2008; Anttila et al., 2009). Assuming that the maximum ambient S typically encountered in warm clouds in the boreal environment is $\sim 0.3\%$, the minimum particle size required for CCN activation would be ~ 85 nm; air masses with predominant S of 0.1–0.15 % would require particles as big as 120–150 nm in diameter for CCN activation. This notion needs to be kept in mind when estimating CCN concentrations from, e.g. DMPS data.

The median aerosol hygroscopicity parameter κ ranged from 0.41 at S of 0.1 % to 0.14 at S of 1.0 % (Table 1; Fig. 6, left panel). This supports the notion previously made by Birmili et al. (2009) that particle hygroscopicity is size-dependent in the region of interest. The variation of κ was also found to decrease with decreasing D_c, as seen by the quartiles, which is in disagreement with the results presented by Swietlicki et al. (2008) and Juranyi et al. (2011). The relationship between κ, D_c and S_{eff} is complex (Eq. 1), and D_c may be used as an indicator of particle hygroscopicity as is; the parameter κ, however, allows for an easier comparison with previous studies, including those with different measurement setups.

Given the overall median κ of 0.22 reported in this study, it can be concluded that the aerosol in the boreal environment is slightly less hygroscopic than the global continental aerosol (an overall average of 0.27 as reported by Pringle et al., 2010). Figure 5 shows that while particles larger than 100 nm in diameter are slightly more hygroscopic than the global continental average, those smaller than 100 nm in diameter are less hy-

groscopic than the global continental mean of κ. Indeed, it seems as though the smaller the particle, the less hygroscopic it is comparative to the global continental mean of κ as seen by the deviation of the points away from the mean global κ line in Fig. 5. The size at which the aerosol particles in Hyytiälä are divided according to differences in CCN-relevant chemical composition coincides with the size typically defining the boundary between Aitken and accumulation modes, i.e. 100 nm (Fig. 5). This notion is of interest since accumulation mode particles are more likely to have been processed by clouds, and, hence, have a higher hygroscopicity. This issue is examined in more detail in the subsequent section. The aerosol at the background station in Southern Finland is also quite less hygroscopic than the European continental aerosol (overall average of 0.36 reported by Pringle et al., 2010b). Being located in a forested rural area in the boreal zone, this lower hygroscopicity is likely explained by the presence of a larger aerosol organic fraction when comparing to other locations within Europe (Zhang et al., 2007). Gunthe et al. (2009) utilised a similar CCNC measurement setup in the Amazonian forest for a month in February and March 2008. For CCN-active fraction of the aerosol the study reported median D_c values of 198 nm and 129 nm for S_{eff} of 0.1 and 0.19 %, respectively, both of which are higher than their corresponding values from this study. Accordingly, κ values reported by the same study for same S_{eff} levels were lower than in this study (Fig. 6, left panel). In fact, for five levels of S_{eff} from 0.1 to 0.82 % Gunthe et al. (2009) reported an overall median value of κ of 0.15, attributing it to a very high organic mass fraction in the Amazonian aerosol, reported to be as high as 90 % for Aitken mode particles. Even though the measurements by Jurányi et al. (2011) were conducted at the high alpine site, mostly in the free troposphere, their reported median κ of 0.20 is very similar to the one reported here, albeit a bit smaller – this is especially true for larger particles (Fig. 6, left panel). Measurements by Levin et al. (2012) in a forested mountainous site in Colorado resulted in an average κ value of 0.16, also smaller than 0.22 reported here. Comparing the hygroscopicity of aerosol among these sites reveals that while aerosol in Hyytiälä exhibits low hygroscopicity with a large organic fraction present, it is more hygroscopic than the aerosol in the Amazon, high

The analysis of size-segregated CCNC data

M. Paramonov et al.

Title Page

Abstract | Introduction

Conclusions | References

Tables | Figures

|◄ | ►|

◄ | ►

Back | Close

Full Screen / Esc

Printer-friendly Version

Interactive Discussion

alpine or forested mountainous environments (Fig. 6, left panel). When the slope values of the linear regression fits in the left panel of Fig. 6 are examined, they point out that the rate of change of aerosol hygroscopicity with size in Hyytiälä is higher than in the Amazon, high alpine or forested mountainous environments, revealing differences in the species of condensing material and the oxidation and aging processes.

The slopes of the linear regression fits in the right panel of Fig. 6 indicate that the increase in hygroscopicity with size in Hyytiälä is highest in the winter and lowest in the summer. One possible reason for this seasonal difference is the notion that in the summer more active SOA formation takes place, resulting in less hygroscopic particles, and in the winter a large fraction of aerosol contains sulphate, especially from the long-range transport. Particle growth is also slower in the winter compared to the summer time due to a smaller amount of condensable vapours.

Sihto et al. (2011) studied aerosol hygroscopic properties for a year at SMEAR II using CCNC coupled with a DMPS and H-TDMA. The reported average D_c values for S_{eff} of 0.4 % derived from both of these setups were higher than 75 nm reported here, stemming from the fact that aerosol populations measured with these two setups include the CCN-inactive fraction, therefore decreasing its overall hygroscopicity. The same explanation applies to the overall average κ of 0.18 as reported by Sihto et al. (2011) for the aerosols of 35, 50, 75 and 110 nm in diameter. A median κ of 0.18 is similar to an average κ of 0.2 reported by Cerully et al. (2011) measured by a CCN chamber at the same location for particles of 40, 60 and 80 nm in diameter. In their study, however, κ did not seem to be dependent on the size.

Having mentioned the variation of D_c and κ with S_{eff}, it is important to note that the overall median values presented for all levels of S_{eff} should be used with caution – they are representative only of the aerosol population which was measured at five specified levels of S_{eff}. In other words, had the CCNC in question been operating at an additional S_{eff} level of, for example, 1.2 %, the overall median values of both D_c and κ would be lower. It is advised that for size-segregated CCNC measurements the presentation of averaged D_c and κ values should always include the levels of S_{eff} at

which the instrument operated; the values may also, of course, be presented for each level of S_{eff} separately.

4.3 The distributions of D_c and κ

Figure 7 shows the distributions of κ as a function of critical diameter D_c. Several features are visible in this figure. For a given S_{eff}, κ is related to D_c with an approximate function of $\kappa \sim D_c^{-3}$, a direct consequence of Eq. (1) assuming that other factors in that equation do not significantly change. The ratio of these $\kappa \sim D_c^{-3}$ relationships scales approximately with $1/\ln^2(S_{eff})$ for different S_{eff} levels, and there is very little variation in the $\kappa \sim D_c^{-3}$ relationship due the functional interrelationship in the fitting procedure.

Perhaps the most interesting feature of Fig. 7 is the evolution of the κ distributions with decreasing S. The measured κ is probably mostly representative of the particle properties near the activation diameter D_c, and thus different S_{eff} values give indication of the frequency of different hygroscopicities as a function of particle diameter. Figure 7 includes the frequency distributions of both κ and D_c, plotted separately on vertical and horizontal axes, and the 25th, 50th and 75th percentiles are plotted directly over the main figure. The κ distributions of the higher S_{eff} measurements show very similar behaviour, with similar distribution width and the median κ close to 0.2. Between the S_{eff} of 0.4 to 0.2 %, the median κ changes significantly and increases to approximately 0.4, and the distribution gets much wider. This widening can be partially explained by decreasing instrumental accuracy at smaller S_{eff}, but more likely it is a result of the much higher variability of the hygroscopicity of larger particles in general. The increase of κ with increasing (critical) diameter is consistent with the change of aerosol population from Aitken to accumulation modes around 100 nm particle diameter, also suggested earlier in Sect. 4.2 (see, e.g. Asmi et al., 2011a, for details of SMEAR II station size distributions). Accumulation mode particles are expected to have been activated at least once as cloud droplets, and thus been subject to cloud processing and other heterogeneous reactions in the aqueous phase. This should increase the contribution of soluble

material, and, hence, the increase in κ should be expected. It is, however, clear that this kind of size-dependent differences in the κ distributions does not support the use of a single κ value regardless of the particle size. One should also notice that even for a single S_{eff}, the κ distributions are close to lognormal in shape, which indicates that arithmetic mean values of κ are probably not the most representative values to use.

Another way to look at the $\kappa - D_{\text{c}}$ distributions is by observing the range of κ for a given critical diameter. For example, looking at the particles near 100 nm critical diameter, one could get κ values from 0.01 to over 1, with possibility of even higher hygroscopicities for S_{eff} lower than the minimum used in this study. Thus, using a single κ value for a given particle size can severely oversimplify the hygroscopicity variability of an aerosol population. Due to the low number of sampled S_{eff}, a 3-D probability density map of κ for each D_{c}, or even a reliable fit for any specific D_{c} are not trivial to derive; however, these results show that even in generally relatively homogeneous regional background conditions the range of κ is large. One should note that the κ values given are not for individual particles, but they represent the aerosol population at sizes near the D_{c} value, and thus the given variability should be considered to be the variability of aerosol populations, not of individual particles.

4.4 Temporal variation

As mentioned previously, the dataset of aerosol CCN activation and hygroscopic properties presented here is unique in a way that it is the first multi-year long-term dataset of ambient measurements in a boreal environment. Figure 8 presents the seasonal variation of D_{c} and κ. The seasonal pattern of aerosol CCN activation and hygroscopicity is only pronounced for larger particles, similar to what has been reported by Levin et al. (2012) for a high-altitude forested site in Colorado. Ambient aerosol populations measured at S_{eff} of 0.1 % seem to be more hygroscopic in winter and less hygroscopic in summer, with February and July being the months showing respective maximum and minimum aerosol hygroscopicity. A minimum of κ in July was also reported by Levin et al. (2012).

It is plausible that the more active SOA formation and the increased organic fraction being the result of increased emissions of the volatile organic compounds (VOCs) from the surrounding boreal environment in the summer are responsible for reducing aerosol hygroscopicity when compared to the winter time. Considering that in Fig. 8 the D_c and κ points for S_{eff} of 0.1 % mirror each other, it is important to point out that the aerosol hygroscopicity can be inferred from the critical diameters alone. The winter peak in aerosol hygroscopicity presented here agrees well with seasonal patterns presented by Pringle et al. (2010) and Sihto et al. (2011) for sites in Germany and Hyytiälä, respectively. Both of these studies also reported aerosol hygroscopicity to be lowest in November, which differs from results presented here (Fig. 8). Since Sihto et al. (2011) employed an H-TDMA to derive hygroscopic properties, the difference in the lowest annual aerosol hygroscopicity may stem from the inclusion of the CCN-inactive fraction in the calculations in the aforementioned study. The pattern in Fig. 8 is clear, and represents the annual hygroscopic properties of the CCN-active fraction only. Also of interest is the fact that the seasonal pattern of D_c presented in Sihto et al. (2011) is evident for all levels of S_{eff} (at S_{eff} of 0.1 % pattern is unclear) and, therefore, for all particle sizes; in the current study the pattern is obvious only for the larger particles and becomes insignificant towards the smaller sizes. There does not seem to be a distinct seasonal pattern for particles smaller than 50 nm – those measured at S_{eff} of 1.0 %. Taking into account that typical levels of ambient S encountered in warm stratiform clouds are low (Pruppacher and Klett, 1997), and, therefore, that particles which activate into cloud drops are the larger ones (> 100 nm), the variation in their chemical composition throughout the year plays a crucial role in cloud formation. The exact reasons for decreased aerosol hygroscopicity during the summer time in Hyytiälä need to be further investigated by a careful comparison with other relevant variables, such as, e.g. concentrations of VOCs.

The analysis of the diurnal behaviour of the aerosol CCN activation and hygroscopic properties revealed that there is no clear diurnal variation of either D_c or κ for largest particles (those with ∼ 150 nm diameter measured at S_{eff} of 0.1 %). When the smallest

particles (< 50 nm) are examined, the absence of the variation is not as clear. When the median values alone are examined, it seems as if particle hygroscopicity is highest around noon and lowest around midnight. The variability and the absolute difference in monthly median values, however, render this variation insignificant and inconclu-
sive. In order to examine the diurnal behaviour in more detail, it was separated by seasons (Fig. 9). Visibly there is most certainly no diurnal variation in aerosol CCN activation and hygroscopic properties in Hyytiälä in autumn and winter. The spring and, especially, summer do exhibit more conclusive diurnal patterns, with both plots showing a decrease in D_c after noon and an increase around midnight. Of interest also is
the variation as demonstrated by the error bars – during the summer time variation in monthly median values is the smallest, pointing out to a more significant pattern in data. Both Sihto et al. (2011) and Cerully et al. (2011) reported diurnal patterns of aerosol hygroscopic properties in Hyytiälä and attributed them to the influence of photochemical reactions and the aging of organics during the sunlight hours. The diurnal
patterns presented here indicate that these processes may well be the reasons for the observed diurnal behaviour, especially considering that the variation is only observed in the spring and summer. The results here agree well with those presented by Cerully et al. (2010), which reported a similar diurnal pattern in κ for particles of 60 nm in diameter measured for two months in the spring in Hyytiälä. While the diurnal pattern
presented here is also similar to the one reported by Sihto et al. (2011), the latter study pointed out that the diurnal variation is more pronounced for larger particles (~ 175 nm in diameter), which is opposite to what has been seen in this analysis. Considering all that has been stated above, it seems that photochemical reactions, aging of the organics, temperature and, possibly, atmospheric nucleation all affect the diurnal behaviour
of CCN activation and hygroscopic properties only for the small, Aitken size aerosol, with a diameter of ~ 50 nm. For larger aerosol (> 100 nm in diameter), the occurrence of these and other processes taking place at different time scales results in no distinguishable effect of photochemistry and temperature on the diurnal behaviour of aerosol CCN activation and hygroscopicity.

Overall, the biogenic emissions and subsequent condensation in the boreal environment of Southern Finland make ambient aerosol of $> 100\,\mathrm{nm}$ in diameter less hygroscopic in the spring and summer time, compared to other seasons; the participation of these emissions in photochemical reactions is responsible for introducing a diurnal pattern in the behaviour of aerosol hygroscopicity in the spring and summer for particles less than 50 nm in diameter. The diminished photochemistry, temperature and biogenic activity in autumn and winter result both in the highest seasonal hygroscopicity of larger ambient aerosol and in the absence of the diurnal variation of aerosol hygroscopicity for particles of any size.

4.5 CCN activation and hygroscopic properties of particles produced by atmospheric new particle formation (NPF)

It has already been shown for a number of locations that NPF locally increases the CCN number concentration (e.g. Kerminen et al., 2012). As a location where atmospheric new particle formation has been studied extensively (e.g. Dal Maso et al., 2005), of interest is to determine the potential difference in D_c and κ between NPF and non-NPF days in Hyytiälä. For this purpose the nucleation event classification based on the DMPS data was used; the nucleation event types mentioned below are described in Dal Maso et al. (2005).

As mentioned in the previous section, the hygroscopicity of particles of $\sim 150\,\mathrm{nm}$ in diameter did not exhibit a diurnal variation in any of the seasons, and the same is true when only the NPF days are considered. During NPF days there is no diurnal variation of D_c and κ and, considering the time it takes for freshly nucleated particles to grow to $\sim 150\,\mathrm{nm}$ in diameter, similar CCN activation and hygroscopic properties are expected for NPF and non-NPF days. For smaller, $\sim 50\,\mathrm{nm}$ particles, the situation is more complicated. Since nucleation events in Hyytiälä occur primarily in the spring (Dal Maso et al., 2005), a subset of 29 spring Type I nucleation events and 53 spring non-event days were selected and analysed (Fig. 10). The diurnal pattern of D_c during non-event days roughly follows the spring pattern depicted in Fig. 9, with a trough

observed around noon; there is, however, a large variation present. The diurnal pattern during the NPF days is also similar in that lowest D_c values are found in the afternoon, and highest between 00:00 and 06:00 UTC + 2 the following day. Nucleation during an event in Hyytiälä typically starts around 10:00 and it takes, on average, 15 h for particles to grow to 50 nm in diameter (Dal Maso et al., 2005). Therefore, if any difference is to be observed in D_c values between NPF and non-NPF days, it should be visible at 01:00 the next day and later. Figure 10 shows that at this time the freshly nucleated particles have grown to be less hygroscopic than they would be in the absence of NPF. While it may be stated that particles produced by NPF and by subsequent growth by vapour condensation may be less hygroscopic due to an increased organic fraction within the aerosol mass, the variability seen in Fig. 10 indicates that this difference between NPF and non-NPF days is not well pronounced and not conclusive. Indeed, if Type II events are included in the analysis, the difference in D_c between 01:00 and 06:00 the following day disappears. Similar is true if summer NPF and non-NPF days are included. Both Ehn et al. (2007) and Sihto et al. (2011) reported an absence of difference in diurnal patterns between NPF and non-NPF days.

What can be concluded from this analysis is that CCN activation and hygroscopic properties of ∼ 50 nm aerosol may be different between NPF and non-NPF days; however, this difference only becomes probable when strong spring nucleation events, for which the growth rates can be calculated with a certain degree of accuracy, are taken into account. Generally speaking, it seems as though particle CCN activation and hygroscopic properties are more affected by the photochemical reactions and atmospheric oxidation of aerosol chemical species, regardless of whether the particles have been produced by NPF or not.

4.6 The inference of ambient aerosol mixing state

Of interest in Table 1 is the overall median maximum activated fraction MAF of 0.95, indicating that for particles of larger sizes on average only 95 % of the total aerosol population were activating into cloud drops. Derived as a result of the non-normalised

fitting procedure of Eq. (2), it represents the fraction of the aerosol population which can be considered CCN-active (Rose et al., 2010). The remaining fraction of 5 %, calculated as 1 – MAF, can then be considered as CCN-inactive fraction or the fraction of the aerosol population that does not activate into cloud drops regardless of how big the particles are or how high the S is inside the CCNC. This partitioning into CCN-active and -inactive fractions may provide insight into the ambient aerosol mixing state; however, such derivation of the mixing state is size-dependent, since for different levels of S_{eff} the function reaches MAF at different sizes. In other words, the point at which the function in Eq. (2) reaches MAF shifts to smaller sizes at increasing S_{eff}. Even though the size range, for which the aerosol mixing state can be estimated, varied with S_{eff}, the median MAF values and the quartiles indicate that there was no significant difference in MAF values among S_{eff} levels. The absence of this difference points out that within the particle size range of ∼ 75–300 nm in diameter the non-normalised method can provide an accurate estimate of the ambient aerosol mixing state.

The quartiles of the overall median MAF indicate that the CCN-inactive fraction may constitute as much as 10 % of the particle number within the size range of ∼ 75–300 nm in diameter or may not be present at all. A closer look at the monthly distribution of the CCN-inactive fraction revealed a seasonal pattern (Fig. 11). The smallest CCN-inactive fraction appears to occur in May, June and July, with the latter being a somewhat unphysical result with a median MAF higher than unity. While this may be explained by the nature of the non-normalised fitting of Eq. (2) and variation in number concentrations at larger sizes, it seems clear that aerosol in the boreal environment is internally mixed in May, June and July, and partially externally mixed throughout the rest of the year. In fact, for May, June and July the median CCN-inactive fraction comprises only 0.2 % of the aerosol population in the abovementioned size range, and for the rest of the year this fraction is 6.6 %. Logically, this seasonal difference also has implications for the choice of method for fitting Eq. (2) to each activation spectrum. If CCN-inactive fraction is very small, the difference in D_c derived from two methods is not as pronounced. Indeed, the regression coefficient R^2 between D_c derived from two methods in May, June

and July is 0.86, and for the rest of year it is 0.57. If the aerosol population in question is internally mixed, it makes no difference whether activation spectra are normalised or not, as both methods produce similar results. If, however, aerosol population is externally mixed, the choice of the method is necessary and it depends on whether one is
5   interested in the whole aerosol population or only in its CCN-active fraction.

It is commonly presumed that the CCN-inactive fraction of the aerosol population consists mainly of insoluble and refractory components, such as mineral dust and black carbon (Gunthe et al., 2009). It can, therefore, be concluded that in Hyytiälä in late spring and early summer the aerosol of $\sim$ 75–300 nm in diameter is internally mixed
10   with low concentrations of CCN-inactive compounds. During the rest of the year the aerosol is not internally mixed and the insoluble and refractory material is present to a larger degree. With black carbon being the most important light-absorbing constituent of the aerosol, this notion is consistent with seasonal cycles of absorption coefficients presented by Virkkula et al. (2011); the study showed the lowest and the highest aver-
15   age absorption coefficients in July and February, respectively. Hyvärinen et al. (2011) and Häkkinen et al. (2012) also reported the lowest aerosol black carbon concentrations in Hyytiälä in the summer time.

5   Conclusions

CCN activation and hygroscopic properties of ambient aerosol have been measured in
20   the boreal environment of Southern Finland with a cloud condensation nuclei counter (CCNC), and this paper presents an in-depth analysis of 29 non-consecutive months of size-segregated measurement data, covering a particle size range of 20–300 nm in diameter and a supersaturation S range of 0.1–1 %. The median critical diameter D_c ranged from 150 nm at S of 0.1 % to 46 nm at S of 1.0 %. For estimating the CCN num-
25   ber concentrations from ambient size distribution measurements in Hyytiälä, a lower limit of 85 nm particle diameter is suggested, assuming an ambient S of < 0.3 % in warm stratiform clouds. The median aerosol hygroscopicity parameter κ ranged from

0.41 at S of 0.1 % to 0.14 at S of 1.0 %, indicating that ambient aerosol in Hyytiälä is slightly less hygroscopic than the modelled global continental average and quite less hygroscopic than the modelled European continental average (Pringle et al., 2010). The lower hygroscopicity in Hyytiälä is likely a result of a large organic fraction present in the aerosol mass comparative to other locations within Europe (Zhang et al., 2007). At the same time, the hygroscopicity itself and its rate of increase with size are larger in the boreal environment than in the Amazon rainforest, high alpine or forested mountainous environments, pointing out to differences in the condensing species, aerosol oxidation and aging. A considerable difference in particle hygroscopicity was found between particles smaller and larger than ∼ 100 nm in diameter, possibly pointing out to the effect of cloud processing increasing κ of particles > 100 nm in diameter. Considering that κ was found to vary with size and that κ distributions were found to be lognormal, the use of a single parameter, mean or median, κ for describing the hygroscopicity of an aerosol population is discouraged.

Throughout the year the hygroscopicity of the smaller, ∼ 50 nm particles did not change, indicating the homogeneity of the CCN-relevant chemical composition. Particles with a diameter of ∼ 150 nm showed a decreased hygroscopicity in the summer, which is possibly attributed to the increased VOC emissions of the surrounding boreal forest. This has direct implications for cloud formation, since typical levels of ambient in-cloud S are very low. For the most part, no diurnal patterns of aerosol hygroscopic properties were found; exceptions to this are weak diurnal patterns of small, ∼ 50 nm particles in the spring and summer. An increase in hygroscopicity around noon was observed for particles of this size, signifying the role of photochemistry and aging of the organics during the sunlight hours. No clear difference in CCN activation and hygroscopic properties was found for aerosol on days with or without atmospheric new particle formation. It was discovered that during all seasons, except summer, a CCN-inactive fraction is present, accounting for as much as 7 % of the total aerosol population, rendering the aerosol as internally mixed in the summer and not internally mixed for the rest of the year.

Title Page

Abstract | Introduction

Conclusions | References

Tables | Figures

◄ | ►|

◄ | ►

Back | Close

Full Screen / Esc

Printer-friendly Version

Interactive Discussion

The analysis and results presented in this paper concentrate primarily on what can be derived and deduced from CCNC data alone. Taking this analysis one step further by using data from other instrumentation at the same location would certainly provide more interesting results and a more detailed insight into aerosol hygroscopic properties in a boreal environment. The concentrations of non-refractory ambient material, such as black carbon, could be used to quantitatively correlate them with the CCN-inactive fraction. The source apportionment of differing aerosol hygroscopicity can be carried out by using the wind direction and backward trajectories data. To demonstrate whether the reduced aerosol hygroscopicity in Hyytiälä is, indeed, a result of heightened organic fraction and emissions, atmospheric mass spectrometry data can be used, and the same applies to sulphate, nitrate and chloride. The representativeness of Hyytiälä in the whole global boreal zone can also be investigated once other long-term datasets obtained with similar measurement setups become available. In general, the results presented here provide a detailed insight into ambient aerosol CCN activation and hygroscopicity in a boreal environment and may serve as a valuable input into the current modelling of aerosol-cloud interactions.

References

Aalto, P.: Atmospheric ultrafine particle measurements, Ph.D. thesis, University of Helsinki, Finland, 40 pp., 2001.
Andreae, M. O. and Rosenfeld, D.: Aerosol-cloud-precipitation interactions – Part 1: The nature and sources of cloud-active aerosols, Earth-Sci. Rev., 89, 13–41, doi:10.1016/j.earscirev.2008.03.001, 2008.

Anttila, T., Vaattovaara, P., Komppula, M., Hyvärinen, A.-P., Lihavainen, H., Kerminen, V.-M., and Laaksonen, A.: Size-dependent activation of aerosols into cloud droplets at a subarctic background site during the second Pallas Cloud Experiment (2nd PaCE): method development and data evaluation, Atmos. Chem. Phys., 9, 4841–4854, doi:10.5194/acp-9-4841-2009, 2009.

Asa-Awuku, A. and Nenes, A.: Effect of solute dissolution kinetics on cloud droplet formation: Extended Köhler theory, J. Geophys. Res., 112, D22201, doi:10.1029/2005JD006934, 2007.

Asmi, A., Wiedensohler, A., Laj, P., Fjaeraa, A.-M., Sellegri, K., Birmili, W., Weingartner, E., Baltensperger, U., Zdimal, V., Zikova, N., Putaud, J.-P., Marinoni, A., Tunved, P., Hansson, H.-C., Fiebig, M., Kivekäs, N., Lihavainen, H., Asmi, E., Ulevicius, V., Aalto, P. P., Swietlicki, E., Kristensson, A., Mihalopoulos, N., Kalivitis, N., Kalapov, I., Kiss, G., de Leeuw, G., Henzing, B., Harrison, R. M., Beddows, D., O'Dowd, C., Jennings, S. G., Flentje, H., Weinhold, K., Meinhardt, F., Ries, L., and Kulmala, M.: Number size distributions and seasonality of submicron particles in Europe 2008–2009, Atmos. Chem. Phys., 11, 5505–5538, doi:10.5194/acp-11-5505-2011, 2011.

Asmi, E., Kivekäs, N., Kerminen, V.-M., Komppula, M., Hyvärinen, A.-P., Hatakka, J., Viisanen, Y., and Lihavainen, H.: Secondary new particle formation in Northern Finland Pallas site between the years 2000 and 2010, Atmos. Chem. Phys., 11, 12959–12972, doi:10.5194/acp-11-12959-2011, 2011.

Baltensperger, U., Gäggeler, H. W., Jost, D. T., Lugauer, M., Schwikowski, M., Weingartner, E., and Seibert, P.: Aerosol climatology at the high alpine site Jungfraujoch, Switzerland, J. Geophys. Res., 102, 19707–19715, doi:10.1029/97JD00928, 1997.

Birmili, W., Schwirn, K., Nowak, A., Petäjä, T., Joutsensaari, J., Rose, D., Wiedensohler, A., Hämeri, K., Aalto, P., Kulmala, M., and Boy, M.: Measurements of humidified particle number size distributions in a Finnish boreal forest: derivation of hygroscopic particle growth factors, Boreal Environ. Res., 14, 458–480, 2009.

Bougiatioti, A., Fountoukis, C., Kalivitis, N., Pandis, S. N., Nenes, A., and Mihalopoulos, N.: Cloud condensation nuclei measurements in the marine boundary layer of the Eastern Mediterranean: CCN closure and droplet growth kinetics, Atmos. Chem. Phys., 9, 7053–7066, doi:10.5194/acp-9-7053-2009, 2009.

Broekhuizen, K., Chang, R.Y.-W., Leaitch, W. R., Li, S.-M., and Abbatt, J. P. D.: Closure between measured and modeled cloud condensation nuclei (CCN) using size-resolved aerosol

Title Page

Abstract | Introduction

Conclusions | References

Tables | Figures

◄ | ►►

◄ | ►

Back | Close

Full Screen / Esc

Printer-friendly Version

Interactive Discussion

compositions in downtown Toronto, Atmos. Chem. Phys., 6, 2513–2524, doi:10.5194/acp-6-2513-2006, 2006.

Cerully, K. M., Raatikainen, T., Lance, S., Tkacik, D., Tiitta, P., Petäjä, T., Ehn, M., Kulmala, M., Worsnop, D. R., Laaksonen, A., Smith, J. N., and Nenes, A.: Aerosol hygroscopicity and CCN activation kinetics in a boreal forest environment during the 2007 EUCAARI campaign, Atmos. Chem. Phys., 11, 12369–12386, doi:10.5194/acp-11-12369-2011, 2011.

Corrigan, C. E. and Novakov, T.: Cloud condensation nucleus activity of organic compounds: a laboratory study, Atmos. Environ., 33, 2661–2668, doi:10.1016/S1352-2310(98)00310-0, 1999.

Covert, D. S., Gras, J. L., Wiedensohler, A., and Stratmann, F.: Comparison of directly measured CCN with CCN modeled from the number-size distribution in the marine boundary layer during ACE 1 at Cape Grim, Tasmania, J. Geophys. Res., 103, 16597–16608, doi:10.1029/98JD01093, 1998.

Cruz, C. N. and Pandis, S. N.: A study of the ability of pure secondary organic aerosol to act as cloud condensation nuclei, Atmos. Environ., 31, 2205–2214, doi:10.1016/S1352-2310(97)00054-X, 1997.

Cubison, M. J., Ervens, B., Feingold, G., Docherty, K. S., Ulbrich, I. M., Shields, L., Prather, K., Hering, S., and Jimenez, J. L.: The influence of chemical composition and mixing state of Los Angeles urban aerosol on CCN number and cloud properties, Atmos. Chem. Phys., 8, 5649–5667, doi:10.5194/acp-8-5649-2008, 2008.

Dal Maso, M., Kulmala, M., Riipinen, I., Wagner, R., Hussein, T., Aalto, P. P., and Lehtinen, K. E. J.: Formation and growth of fresh atmospheric aerosols: eight years of aerosol size distribution data from SMEAR II, Hyytiälä, Finland, Boreal Environ. Res., 10, 323–336, 2005.

Dusek, U., Frank, G. P., Hildebrandt, L., Curtius, J., Schneider, J., Walter, S., Chand, D., Drewnick, F., Hings, S., Jung, D., Borrmann, S., and Andreae, M. O.: Size matters more than chemistry for cloud-nucleating ability of aerosol particles, Science, 312, 1375–1378, doi:10.1126/science.1125261, 2006.

Ehn, M., Petäjä, T., Aufmhoff, H., Aalto, P., Hämeri, K., Arnold, F., Laaksonen, A., and Kulmala, M.: Hygroscopic properties of ultrafine aerosol particles in the boreal forest: diurnal variation, solubility and the influence of sulfuric acid, Atmos. Chem. Phys., 7, 211–222, doi:10.5194/acp-7-211-2007, 2007.

Title Page

Abstract | Introduction

Conclusions | References

Tables | Figures

|◄ | ►|

◄ | ►

Back | Close

Full Screen / Esc

Printer-friendly Version

Interactive Discussion

Engelhart, G. J., Asa-Awuku, A., Nenes, A., and Pandis, S. N.: CCN activity and droplet growth kinetics of fresh and aged monoterpene secondary organic aerosol, Atmos. Chem. Phys., 8, 3937–3949, doi:10.5194/acp-8-3937-2008, 2008.

Ervens, B., Cubison, M. J., Andrews, E., Feingold, G., Ogren, J. A., Jimenez, J. L., Quinn, P. K., Bates, T. S., Wang, J., Zhang, Q., Coe, H., Flynn, M., and Allan, J. D.: CCN predictions using simplified assumptions of organic aerosol composition and mixing state: a synthesis from six different locations, Atmos. Chem. Phys., 10, 4795–4807, doi:10.5194/acp-10-4795-2010, 2010.

Finlayson-Pitts, B. J. and Pitts Jr., J. N.: Tropospheric air pollution: Ozone, airborne toxics, polycyclic aromatic hydrocarbons, and particles, Science, 276, 1045–1052, doi:10.1126/science.276.5315.1045, 1997.

Fitzgerald, J. W., Hoppel, W. A., and Vietti, M. A.: The size and scattering coefficient of urban aerosol particles at Washington, DC, as a function of relative humidity, J. Atmos. Sci., 39, 1838–1852, doi:10.1175/1520-0469(1982)039<1838:TSASCO>2.0.CO;2, 1982.

Forster, P., Ramaswamy, V., Artaxo, P., Berntsen, T., Betts, R., Fahey, D. W., Haywood, J., Lean, J., Lowe, D. C., Myhre, G., Nganga, J., Prinn, R., Raga, G., Schulz, M., and Van Dorland, R.: Changes in Atmospheric Constituents and in Radiative Forcing, in: Climate Change 2007: The Physical Science Basis. Contribution of Working Group I to the Fourth Assessment Report of the Intergovernmental Panel on Climate Change, edited by: Solomon, S., Qin, D., Manning, M., Chen, Z., Marquis, M., Averyt, K. B., Tignor, M., and Miller, H. L., Cambridge University Press, Cambridge, UK and New York, NY, USA, 2007.

Gras, J. L.: Cloud condensation nuclei over the Southern Ocean, Geophys. Res. Lett., 17, 1565–1567, doi:10.1029/GL017i010p01565, 1990.

Gunthe, S. S., King, S. M., Rose, D., Chen, Q., Roldin, P., Farmer, D. K., Jimenez, J. L., Artaxo, P., Andreae, M. O., Martin, S. T., and Pöschl, U.: Cloud condensation nuclei in pristine tropical rainforest air of Amazonia: size-resolved measurements and modeling of atmospheric aerosol composition and CCN activity, Atmos. Chem. Phys., 9, 7551–7575, doi:10.5194/acp-9-7551-2009, 2009.

Häkkinen, S. A. K., Äijälä, M., Lehtipalo, K., Junninen, H., Backman, J., Virkkula, A., Nieminen, T., Vestenius, M., Hakola, H., Ehn, M., Worsnop, D. R., Kulmala, M., Petäjä, T., and Riipinen, I.: Long-term volatility measurements of submicron atmospheric aerosol in Hyytiälä, Finland, Atmos. Chem. Phys., 12, 10771–10786, doi:10.5194/acp-12-10771-2012, 2012.

Title Page

Abstract | Introduction

Conclusions | References

Tables | Figures

◄◄ | ►►

◄ | ►

Back | Close

Full Screen / Esc

Printer-friendly Version

Interactive Discussion

Hari, P. and Kulmala, M.: Station for measuring Ecosystem–Atmosphere Relations (SMEAR II), Boreal Environ. Res., 10, 315–322, 2005.

Hatakka, J., Aalto, T., Aaltonen, V., Aurela, M., Hakola, H., Komppula, M., Laurila, T., Lihavainen, H., Paatero, J., Salminen, K., and Viisanen, Y.: Overview of the atmospheric research activities and results at Pallas GAW station, Boreal Environ. Res., 8, 365–383, 2003.

Hinds, W. C. (Eds.): Aerosol Technology: Properties, Behavior, and Measurement of Airborne Particles, John Wiley & Sons, New York, USA, 1999.

Hobbs, P. V., Stith, J. L., and Radke, L. F.: Cloud-active nuclei from coal-fired electric power plants and their interactions with clouds, J. Appl. Meteorol., 19, 439–451, doi:10.1175/1520-0450(1980)019<0439:CANFCF>2.0.CO;2, 1980.

Hyvärinen, A.-P., Kolmonen, P., Kerminen, V.-M., Virkkula, A., Leskinen, A., Komppula, M., Hatakka, J., Burkhart, J., Stohl, A., Aalto, P., Kulmala, M., Lehtinen, K. E. J., Viisanen, Y., and Lihavainen, H.: Aerosol black carbon at five background measurement sites over Finland, a gateway to the Arctic, Atmos. Environ., 45, 4042–4050, doi:10.1016/j.atmosenv.2011.04.026, 2011.

Jinhuan, Q. and Liquan, Y.: Variation characteristics of atmospheric aerosol optical depths and visibility in North China during 1980–1994, Atmos. Environ., 34, 603–609, doi:10.1016/S1352-2310(99)00173-9, 2000.

Jurányi, Z., Gysel, M., Weingartner, E., Bukowiecki, N., Kammermann, L., and Baltensperger, U.: A 17 month climatology of the cloud condensation nuclei number concentration at the high alpine site Jungfraujoch, J. Geophys. Res., 116, D10204, doi:10.1029/2010JD015199, 2011.

Kammermann, L., Gysel, M., Weingartner, E., and Baltensperger, U.: 13-month climatology of the aerosol hygroscopicity at the free tropospheric site Jungfraujoch (3580 m a.s.l.), Atmos. Chem. Phys., 10, 10717-10732, doi:10.5194/acp-10-10717-2010, 2010.

Kandler, K. and Shütz, L.: Climatology of the average water-soluble volume fraction of atmospheric aerosol, Atmos. Res., 83, 77–92, doi:10.1016/j.atmosres.2006.03.004, 2007.

Kerminen, V.-M., Paramonov, M., Anttila, T., Riipinen, I., Fountoukis, C., Korhonen, H., Asmi, E., Laakso, L., Lihavainen, H., Swietlicki, E., Svenningsson, B., Asmi, A., Pandis, S. N., Kulmala, M., and Petäjä, T.: Cloud condensation nuclei production associated with atmospheric nucleation: a synthesis based on existing literature and new results, Atmos. Chem. Phys., 12, 12037–12059, doi:10.5194/acp-12-12037-2012, 2012.

Title Page

Abstract | Introduction

Conclusions | References

Tables | Figures

|◀ | ▶|

◀ | ▶

Back | Close

Full Screen / Esc

Printer-friendly Version

Interactive Discussion

Khvorostyanov, V. I. and Curry, J. A.: Refinements to the Köhler's theory of aerosol equilib-
rium radii, size spectra, and droplet activation: Effects of humidity and insoluble fraction, J.
Geophys. Res., 112, D05206, doi:10.1029/2006JD007672, 2007.

Köhler, H.: The nucleus in and the growth of hygroscopic droplets, T. Faraday Soc., 43, 1152,
doi:10.1039/TF9363201152, 1936.

Komppula, M., Lihavainen, H., Kerminen, V.-M., Kulmala, M., and Viisanen, Y.: Measurements
of cloud droplet activation of aerosol particles at a clean subarctic background site, J. Geo-
phys. Res., 110, D06204, doi:10.1029/2004JD005200, 2005.

Kulmala, M., Laaksonen, A., Korhonen, P., Vesala, T., Anonen, T., and Barrett, J. C.: The effect
of atmospheric nitric acid vapor on cloud condensation nucleus activation, J. Geophys. Res.,
98, 22949–22958, doi:10.1029/93JD02070, 1993.

Leaitch, W. R., Isaac, G. A., Strapp, J. W., Banic, C. M., and Wiebe, H. A.: The relationship
between cloud droplet number concentrations and anthropogenic pollution: observations and
climate implications, J. Geophys. Res., 97, 2463–2474, doi:10.1029/91JD02739, 1992.

Leskinen, A., Portin, H., Komppula, M., Miettinen, P., Arola, A., Lihavainen, H., Hatakka, J.,
Laaksonen, A., and Lehtinen, K. E. J.: Overview of the research activities and results at
Puijo semi-urban measurement station, Boreal Environ. Res., 14, 576–590, 2009.

Levin, E. J. T., Prenni, A. J., Petters, M. D., Kreidenweis, S. M., Sullivan, R. C., At-
wood, S. A., Ortega, J., DeMott, P. J., and Smith, J. N.: An annual cycle of size-resolved
aerosol hygroscopicity at a forested site in Colorado, J. Geophys. Res., 117, D06201,
doi:10.1029/2011JD016854, 2012.

Lihavainen, H., Kerminen, V.-M., Komppula, M., Hatakka, J., Aaltonen, V., Kulmala, M.,
and Viisanen, Y.: Production of "potential" cloud condensation nuclei associated with
atmospheric new-particle formation in northern Finland, J. Geophys. Res., 108, 4782,
doi:10.1029/2003JD003887, 2003.

Lihavainen, H., Kerminen, V.-M., Komppula, M., Hyvärinen, A.-P., Laakia, J., Saarikoski, S.,
Makkonen, U., Kivekäs, N., Hillamo, R., Kulmala, M., and Viisanen, Y.: Measurements of the
relation between aerosol properties and microphysics and chemistry of low level liquid water
clouds in Northern Finland, Atmos. Chem. Phys., 8, 6925–6938, doi:10.5194/acp-8-6925-
2008, 2008.

Lohmann, U. and Feichter, J.: Global indirect aerosol effects: a review, Atmos. Chem. Phys., 5,
715–737, doi:10.5194/acp-5-715-2005, 2005.

Title Page

Abstract | Introduction

Conclusions | References

Tables | Figures

|◀ | ▶|

◀ | ▶

Back | Close

Full Screen / Esc

Printer-friendly Version

Interactive Discussion

McCormick, R. and Ludwig, J. H.: Climate modification by atmospheric aerosols, Science, 156, 1358–1359, 1967.

McFiggans, G., Artaxo, P., Baltensperger, U., Coe, H., Facchini, M. C., Feingold, G., Fuzzi, S., Gysel, M., Laaksonen, A., Lohmann, U., Mentel, T. F., Murphy, D. M., O'Dowd, C. D., Snider, J. R., and Weingartner, E.: The effect of physical and chemical aerosol properties on warm cloud droplet activation, Atmos. Chem. Phys., 6, 2593–2649, doi:10.5194/acp-6-2593-2006, 2006.

Merikanto, J., Spracklen, D. V., Mann, G. W., Pickering, S. J., and Carslaw, K. S.: Impact of nucleation on global CCN, Atmos. Chem. Phys., 9, 8601–8616, doi:10.5194/acp-9-8601-2009, 2009.

Nyeki, S., Li, F., Weingartner, E., Streit, N., Colbeck, I., Gäggeler, H. W., and Baltensperger, U.: The background aerosol size distribution in the free troposphere: An analysis of the annual cycle at a high-alpine site, J. Geophys. Res., 103, 31749–31761, doi:10.1029/1998JD200029, 1998.

Padró, L. T., Asa-Awuku, A., Morrison, R., and Nenes, A.: Inferring thermodynamic properties from CCN activation experiments: single-component and binary aerosols, Atmos. Chem. Phys., 7, 5263–5274, doi:10.5194/acp-7-5263-2007, 2007.

Petters, M. D. and Kreidenweis, S. M.: A single parameter representation of hygroscopic growth and cloud condensation nucleus activity, Atmos. Chem. Phys., 7, 1961–1971, doi:10.5194/acp-7-1961-2007, 2007.

Petters, M. D., Prenni, A. J., Kreidenweis, S. M., and DeMott, P. J.: On measuring the critical diameter of cloud condensation nuclei using mobility selected aerosol, Aerosol Sci. Tech., 41, 907–913, doi:10.1080/02786820701557214, 2007.

Pringle, K. J., Tost, H., Pozzer, A., Pöschl, U., and Lelieveld, J.: Global distribution of the effective aerosol hygroscopicity parameter for CCN activation, Atmos. Chem. Phys., 10, 5241–5255, doi:10.5194/acp-10-5241-2010, 2010.

Prisle, N. L., Raatikainen, T., Laaksonen, A., and Bilde, M.: Surfactants in cloud droplet activation: mixed organic-inorganic particles, Atmos. Chem. Phys., 10, 5663–5683, doi:10.5194/acp-10-5663-2010, 2010.

Pruppacher, H. and Klett, J.: Microphysics of clouds and precipitation, Atmospheric and oceanographic sciences library; v. 18, includes bibliographical references and index Previous edn., 1978 "With an introduction to cloud chemistry and cloud electricity", Kluwer Academic Publishers, Dordrecht, London, 1997.

Title Page

Abstract | Introduction

Conclusions | References

Tables | Figures

|◀ | ▶|

◀ | ▶

Back | Close

Full Screen / Esc

Printer-friendly Version

Interactive Discussion

Reutter, P., Su, H., Trentmann, J., Simmel, M., Rose, D., Gunthe, S. S., Wernli, H., Andreae, M. O., and Pöschl, U.: Aerosol- and updraft-limited regimes of cloud droplet formation: influence of particle number, size and hygroscopicity on the activation of cloud condensation nuclei (CCN), Atmos. Chem. Phys., 9, 7067–7080, doi:10.5194/acp-9-7067-2009, 2009.

Rissler, J., Pagels, J., Swietlicki, E., Wierzbicka, A., Strand, M., Lillieblad, L., Sanati, M., and Bohgard, M.: Hygroscopic behavior of aerosol particles emitted from biomass fired grate boilers, Aerosol. Sci. Tech., 39, 919–930, doi:10.1080/02786820500331068, 2005.

Rissler, J., Vestin, A., Swietlicki, E., Fisch, G., Zhou, J., Artaxo, P., and Andreae, M. O.: Size distribution and hygroscopic properties of aerosol particles from dry-season biomass burning in Amazonia, Atmos. Chem. Phys., 6, 471–491, doi:10.5194/acp-6-471-2006, 2006.

Rissman, T. A., VenReken, T. M., Wang, J., Gasparini, R., Collins, D. R., Jonsson, H. H., Brechtel, F. J., Flagan, R. C., and Seinfeld, J. H.: Characterization of ambient aerosol from measurements of cloud condensation nuclei during the 2003 Atmospheric Radiation Measurement Aerosol Intensive Observational Period at the Southern Great Plains site in Oklahoma, J. Geophys. Res., 111, D05S11, doi:10.1029/2004JD005695, 2006.

Roberts, G. C. and Nenes, A.: A continuous-flow streamwise thermal-gradient CCN chamber for atmospheric measurements, Aerosol Sci. Tech., 39, 206–221, doi:10.1080/027868290913988, 2005.

Roberts, G. C., Artaxo, P., Zhou, J., Swietlicki, E., and Andreae, M. O.: Sensitivity of CCN spectra on chemical and physical properties of aerosol: A case study from the Amazon Basin, J. Geophys. Res., 107, 8070, doi:10.1029/2001JD000583, 2002.

Roberts, G., Mauger, G., Hadley, O., and Ramanathan, V.: North American and Asian aerosols over the eastern Pacific Ocean and their role in regulating cloud condensation nuclei, J. Geophys. Res., 111, D13205, doi:10.1029/2005JD006661, 2006.

Rose, D., Gunthe, S. S., Mikhailov, E., Frank, G. P., Dusek, U., Andreae, M. O., and Pöschl, U.: Calibration and measurement uncertainties of a continuous-flow cloud condensation nuclei counter (DMT-CCNC): CCN activation of ammonium sulfate and sodium chloride aerosol particles in theory and experiment, Atmos. Chem. Phys., 8, 1153–1179, doi:10.5194/acp-8-1153-2008, 2008.

Rose, D., Nowak, A., Achtert, P., Wiedensohler, A., Hu, M., Shao, M., Zhang, Y., Andreae, M. O., and Pöschl, U.: Cloud condensation nuclei in polluted air and biomass burning smoke near the mega-city Guangzhou, China – Part 1: Size-resolved measurements and implications for

Title Page

Abstract | Introduction

Conclusions | References

Tables | Figures

|◀ | ▶|

◀ | ▶

Back | Close

Full Screen / Esc

Printer-friendly Version

Interactive Discussion

the modeling of aerosol particle hygroscopicity and CCN activity, Atmos. Chem. Phys., 10, 3365–3383, doi:10.5194/acp-10-3365-2010, 2010.

Seaton, A., MacNee, W., Donaldson, K., and Godden, D.: Particulate air pollution and acute health effects, Lancet, 345, 176–178, doi:10.1016/S0140-6736(95)90173-6, 1995.

Seinfeld, J. H. and Pandis, S. N. (Eds.): Atmospheric chemistry and physics: from air pollution to climate change, 2nd edn., John Wiley & Sons, New York, USA, 2006.

Sihto, S.-L., Mikkilä, J., Vanhanen, J., Ehn, M., Liao, L., Lehtipalo, K., Aalto, P. P., Duplissy, J., Petäjä, T., Kerminen, V.-M., Boy, M., and Kulmala, M.: Seasonal variation of CCN concentrations and aerosol activation properties in boreal forest, Atmos. Chem. Phys., 11, 13269–13285, doi:10.5194/acp-11-13269-2011, 2011.

Snider, J. R. and Brenguier, J.-L.: Cloud condensation nuclei and cloud droplet measurements during ACE-2, Tellus B, 52, 828–842, doi:10.1034/j.1600-0889.2000.00044.x, 2000.

Snider, J. R., Guibert, S., Brenguier, J.-L., and Putaud, J.-P.: Aerosol activation in marine stratocumulus clouds: 2. Köhler and parcel theory closure studies, J. Geophys. Res., 108, 8629, doi:10.1029/2002JD002692, 2003.

Sogacheva, L., Dal Maso, M., Kerminen, V.-M., and Kulmala, M.: Probability of nucleation events and aerosol particle concentration in different air mass types arriving at Hyytiälä, southern Finland, based on back trajectories analysis, Boreal Environ. Res., 10, 479–491, 2005.

Su, H., Rose, D., Cheng, Y. F., Gunthe, S. S., Massling, A., Stock, M., Wiedensohler, A., Andreae, M. O., and Pöschl, U.: Hygroscopicity distribution concept for measurement data analysis and modeling of aerosol particle mixing state with regard to hygroscopic growth and CCN activation, Atmos. Chem. Phys., 10, 7489–7503, doi:10.5194/acp-10-7489-2010, 2010.

Svenningsson, I. B., Hansson, H. C., Wiedensohler, A., Ogren, J. A., Noone, K. J., and Hallberg, A.: Hygroscopic growth of aerosol-particles in the Po Valley, Tellus B, 44, 556–569, doi:10.1034/j.1600-0889.1992.t01-1-00009.x, 1992.

Swietlicki, E., Hansson, H.-C., Hämeri, K., Svenningsson, B., Massling, A., McFiggans, G., McMurry, P. H., Petäjä, T., Tunved, P., Gysel, M., Topping, D., Weingartner, E., Baltensperger, U., Rissler, J., Wiedensohler, A., and Kulmala, M.: Hygroscopic properties of submicrometer atmospheric aerosol particles measured with H-TDMA instruments in various environments – a review, Tellus B, 60, 432–469, doi:10.1111/j.1600-0889.2008.00350.x, 2008.

Twomey, S.: Pollution and planetary albedo, Atmos. Environ., 8, 1251–1256, doi:10.1016/0004-6981(74)90004-3, 1974.

Title Page

Abstract | Introduction

Conclusions | References

Tables | Figures

|◄ | ►|

◄ | ►

Back | Close

Full Screen / Esc

Printer-friendly Version

Interactive Discussion

Twomey, S. and Wojciechowski, T. A.: Observations of geographical variation of cloud nuclei, J. Atmos. Sci., 26, 684–688, doi:10.1175/1520-0469(1969)26<648:OOTGVO>2.0.CO;2, 1969.

Van Pinxteren, D., Birmili, W., Fahlbusch, B., Fomba, W., Gnauk, T., Iinuma, Y., Mertes, S., Dieckmann, K., Merkel, M., Müller, C., Müller, K., Poulain, L., Spindler, G., Schäfer, M., Stratmann, F., Tilgner, A., Schöne, L., Bräuer, P., Weinhold, K., Wiedensohler, A., Zhijun, W., Borrmann, S., Harris, E., Roth, A., Schneider, J., Sinha, B., George, I., Heard, D., Whalley, L., D'Anna, B., George, C., Müller, M., Haunold, W., Engel, A., Wéber, A., Amedro, D., Fittschen, C., Schoemaecker, C., Collett, J., Lee, T., and Herrmann, H.: Hill Cap Cloud Thuringia 2010 (HCCT-2010): Overview and highlight results, European Aerosol Conference, Granada, Spain, 2–7 September 2012, SS02S1O01, 2012.

VanReken, T. M., Rissman, T. A., Roberts, G. C., Varutbangkul, V., Jonsson, H. H., Flagan, R. C., and Seinfeld, J. H.: Toward aerosol/cloud condensation nuclei (CCN) closure during CRYSTAL-FACE, J. Geophys. Res., 108, 4633, doi:10.1029/2003JD003582, 2003.

Virkkula, A., Backman, J., Aalto, P. P., Hulkkonen, M., Riuttanen, L., Nieminen, T., dal Maso, M., Sogacheva, L., de Leeuw, G., and Kulmala, M.: Seasonal cycle, size dependencies, and source analyses of aerosol optical properties at the SMEAR II measurement station in Hyytiälä, Finland, Atmos. Chem. Phys., 11, 4445–4468, doi:10.5194/acp-11-4445-2011, 2011.

Wang, J., Lee, Y.-N., Daum, P. H., Jayne, J., and Alexander, M. L.: Effects of aerosol organics on cloud condensation nucleus (CCN) concentration and first indirect aerosol effect, Atmos. Chem. Phys., 8, 6325–6339, doi:10.5194/acp-8-6325-2008, 2008.

Wang, J., Cubison, M. J., Aiken, A. C., Jimenez, J. L., and Collins, D. R.: The importance of aerosol mixing state and size-resolved composition on CCN concentration and the variation of the importance with atmospheric aging of aerosols, Atmos. Chem. Phys., 10, 7267–7283, doi:10.5194/acp-10-7267-2010, 2010.

Zhang, Q., Jimenez, J. L., Canagaratna, M. R., Allan, J. D., Coe, H., Ulbrich, I., Alfarra, M. R., Takami, A., Middlebrook, A. M., Sun, Y. L., Dzepina, K., Dunlea, E., Docherty, K., DeCarlo, P. F., Salcedo, D., Onasch, T., Jayne, J. T., Miyoshi, T., Shimono, A., Hatakeyama, S., Takegawa, N., Kondo, Y., Schneider, J., Drewnick, F., Borrmann, S., Weimer, S., Demerjian, K., Williams, P., Bower, K., Bahreini, R., Cottrell, L., Griffin, R. J., Rautiainen, J., Sun, J. Y., Zhang, Y. M., and Worsnop, D. R.: Ubiquity and dominance of oxygenated species

in organic aerosols in anthropogenically-influenced Northern Hemisphere midlatitudes, Geophys. Res. Lett., 34, L13801, doi:10.1029/2007GL029979, 2007.

Table 1. Number of spectra, the results of the normalised and non-normalised fitting of Eq. (2), the related terms and the derived parameters of D_c and κ used in this study. For parameters shown are the median values, with 25th and 75th percentile values included in the square brackets. Data shown separately for each supersaturation S_{eff} level, as well as for the whole dataset.

S_{eff} # of spectra	0.1 % 9332	0.2 % 9308	0.4 % 9274	0.6 % 9224	1.0 % 9262	ALL 46 400
Eq. (2) fit RMSE, normalised method	0.08 [0.06; 0.11]	0.12 [0.10; 0.15]	0.14 [0.12; 0.17]	0.16 [0.13; 0.18]	0.18 [0.15; 0.21]	0.14 [0.10; 0.18]
Eq. (2) fit RMSE, non-normalised method	0.08 [0.06; 0.10]	0.09 [0.07; 0.12]	0.10 [0.08; 0.13]	0.11 [0.08; 0.13]	0.12 [0.09; 0.15]	0.10 [0.07; 0.13]
a, non-normalised method	0.46 [0.41; 0.52]	0.47 [0.45; 0.50]	0.48 [0.46; 0.50]	0.48 [0.46; 0.50]	0.47 [0.46; 0.49]	0.47 [0.45; 0.50]
MAF, non-normalised method	0.92 [0.82; 1.04]	0.94 [0.89; 1.00]	0.95 [0.91; 1.00]	0.95 [0.91; 1.00]	0.95 [0.91; 0.99]	0.95 [0.90; 1.00]
D_c(nm), normalised method	174.39 [152.93; 195.89]	114.93 [102.13; 133.42]	88.27 [79.28; 104.67]	73.49 [65.61; 91.13]	57.20 [50.05; 79.67]	97.52 [72.03; 136.12]
D_c(nm), non-normalised method	150.46 [129.81; 175.37]	96.35 [87.40; 106.24]	74.82 [68.73; 80.19]	61.36 [56.59; 65.68]	45.53 [42.19; 48.44]	75.24 [56.89; 104.52]
κ, normalised method	0.26 [0.18; 0.39]	0.23 [0.15; 0.33]	0.13 [0.07; 0.17]	0.10 [0.05; 0.14]	0.07 [0.02; 0.11]	0.13 [0.08; 0.23]
κ, non-normalised method	0.41 [0.26; 0.64]	0.39 [0.29; 0.52]	0.21 [0.17; 0.27]	0.17 [0.13; 0.21]	0.14 [0.12; 0.18]	0.22 [0.15; 0.36]
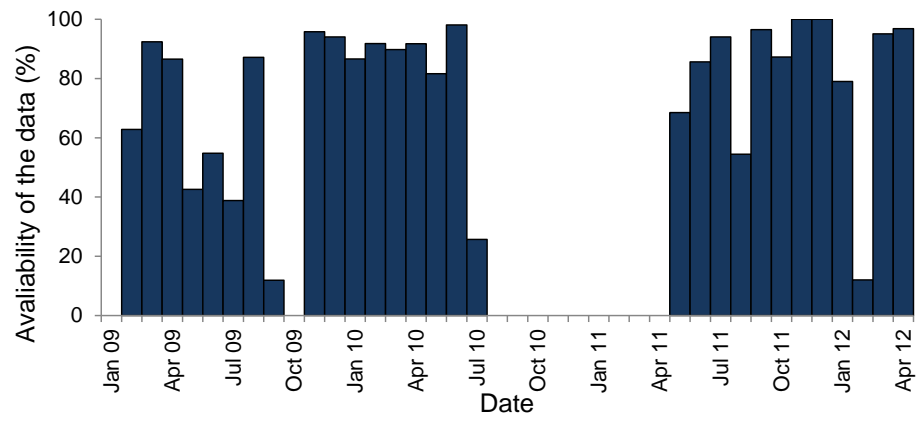
Fig. 1. Monthly availability of CCNC data.
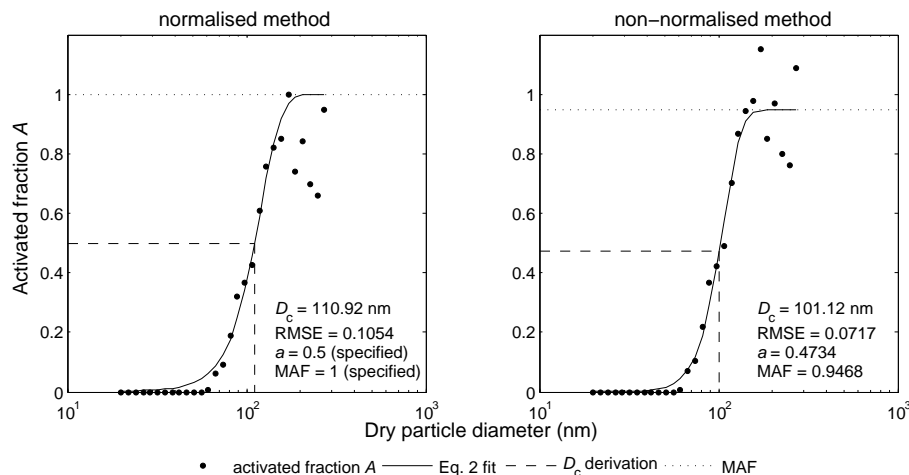
Fig. 2. A sample CCN efficiency spectrum measured on 24 June 2009 from 20:02:03 to 20:23:13 UTC+2, and two ways of determining D_c. Left panel: normalised method; right panel: non-normalised method. Both panels show the calculated D_c, a root mean square error (RMSE) of the fit, a and the maximum activated fraction MAF. Note, that in the normalised method a and MAF were assigned values of 0.5 and 1, respectively; in the non-normalised method these values were allowed to vary.
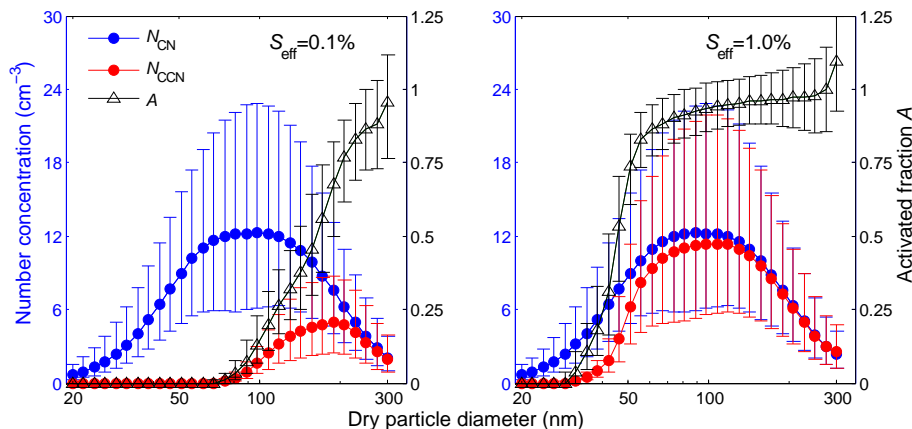
Fig. 3. Median N_{CN}, N_{CCN} and A per size bin for the whole dataset for two levels of supersaturation S_{eff}. Left panel: $S_{eff} = 0.1\%$; right panel: $S_{eff} = 1.0\%$. Error bars show 25th and 75th percentiles.
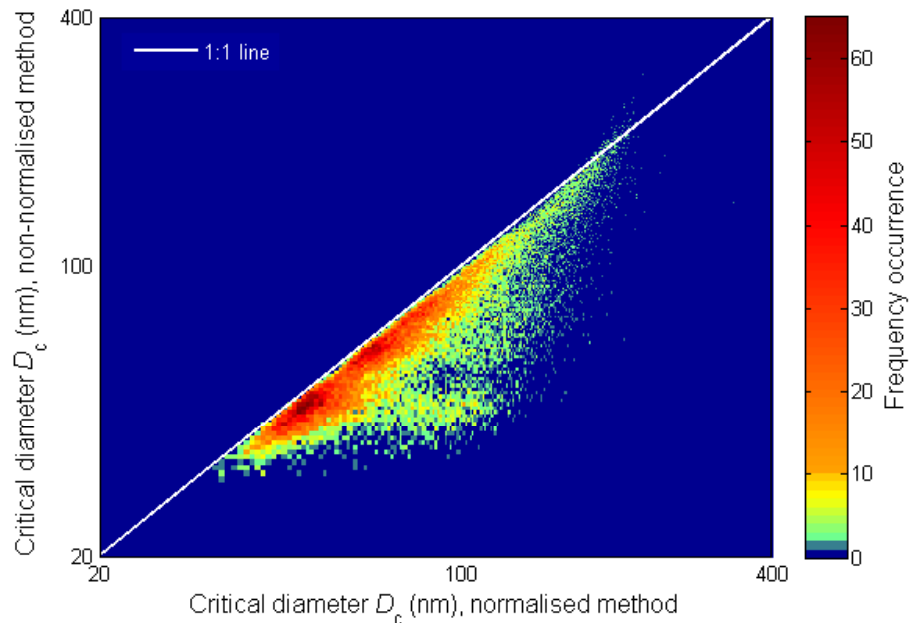
Fig. 4. A contour plot frequency distribution of the critical diameters D_c calculated by two methods. Each grid cell is 1×1 nm. Included in the figure is the $1:1$ line (white line).
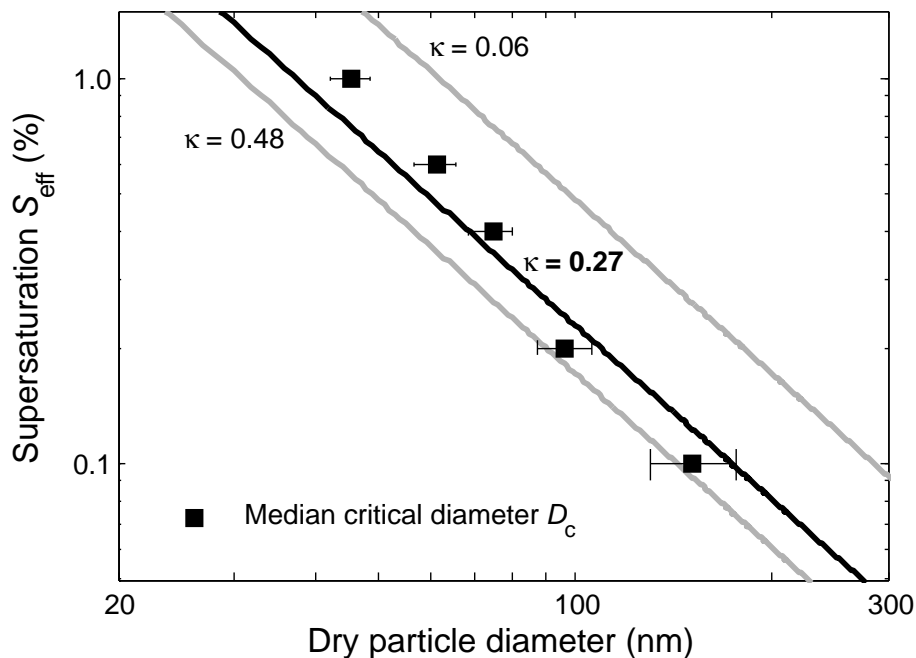
Fig. 5. Relationship between particle dry size (taken as D_c) and critical supersaturation S_{eff}. The black and grey lines correspond to the global continental mean κ of 0.27 ± 0.21 as reported by Pringle et al. (2010), and the error bars are 25th and 75th percentiles of median D_c.
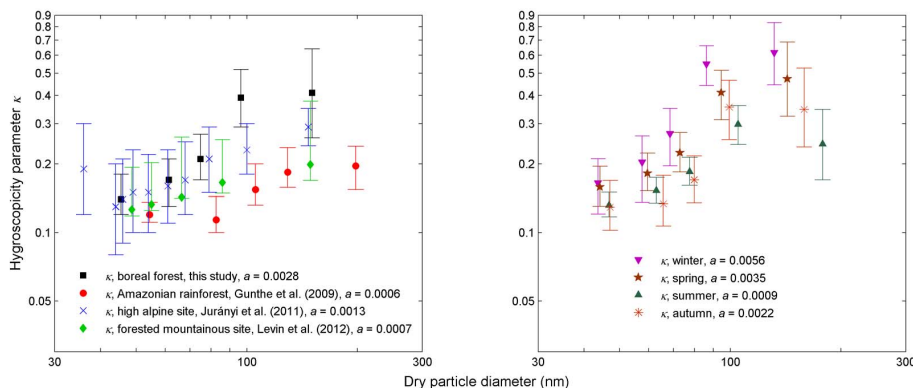
Fig. 6. Relationship between particle dry size (taken as D_c) and hygroscopicity parameter κ. Left panel shows the comparison among sites; right panel shows comparison among seasons for Hyytiälä. Both panels show the median values with error bars being 25th and 75th percentiles (for Gunthe et al., 2009 percentiles estimated from the original publication). Legend entries also indicate the slope of the linear regression $y = ax + b$ fit.

Title Page

Abstract | Introduction

Conclusions | References

Tables | Figures

|◄ | ►|

◄ | ►

Back | Close

Full Screen / Esc

Printer-friendly Version

Interactive Discussion
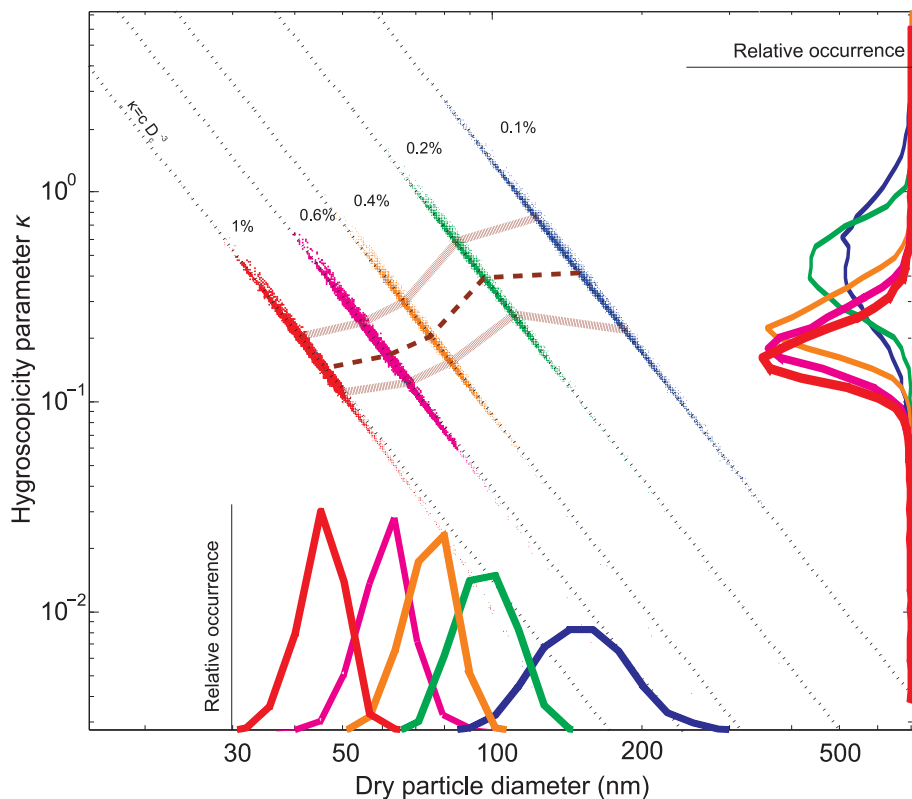
Fig. 7. Distributions of κ values as a function of dry particle diameter (taken as D_c). The different colours indicate different S_{eff} levels, and the sides of the figure show relative occurrence of κ (vertical axis) and D_c (horizontal axis) calculated with log-equal bins. The dashed lines show the 25th, 50th and 75th percentiles of each supersaturation distribution. The gray dotted lines show expected $\kappa \sim D_c^{-3}$ relationship for each S_{eff} level.
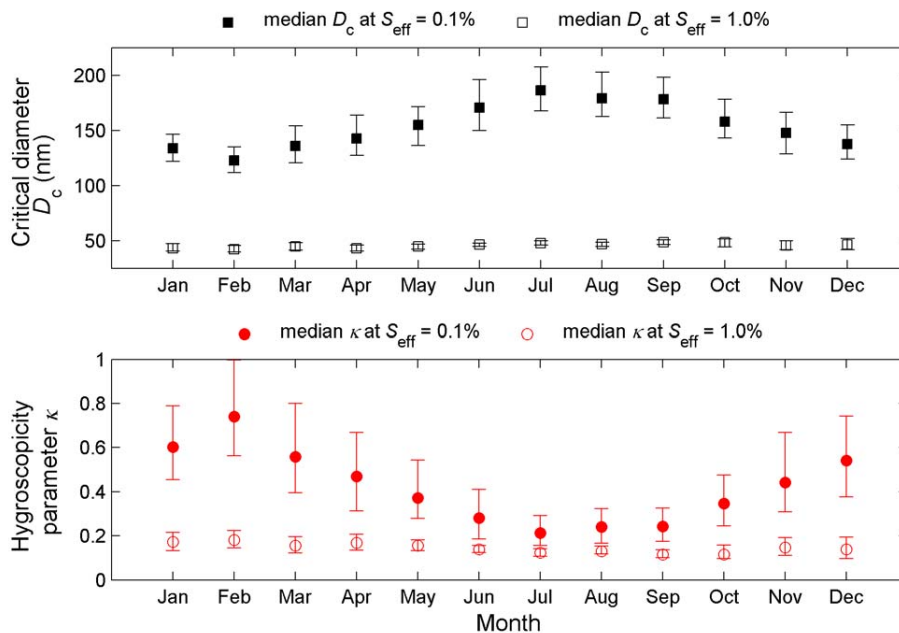
Fig. 8. Monthly median critical diameters D_c (top) and hygroscopicity parameters κ (bottom), shown for two levels of supersaturation S_{eff}. Error bars are 25th and 75th percentiles.
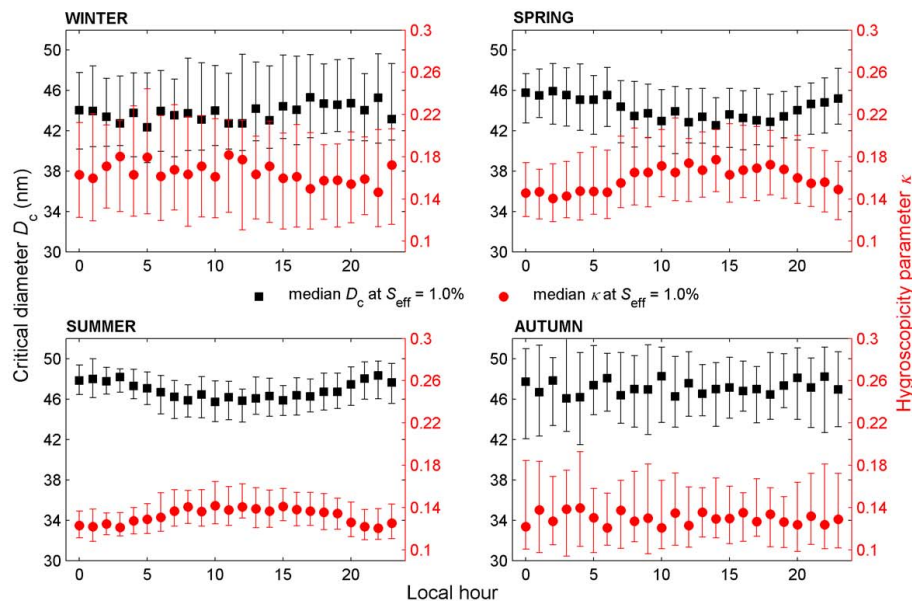
Fig. 9. Hourly median critical diameters D_c (black) and hygroscopicity parameters κ (red), shown for S_{eff} of 1.0 % and separated by seasons. Error bars are 25th and 75th percentiles.

Title Page

Abstract | Introduction

Conclusions | References

Tables | Figures

◄ | ►►

◄ | ►

Back | Close

Full Screen / Esc

Printer-friendly Version

Interactive Discussion
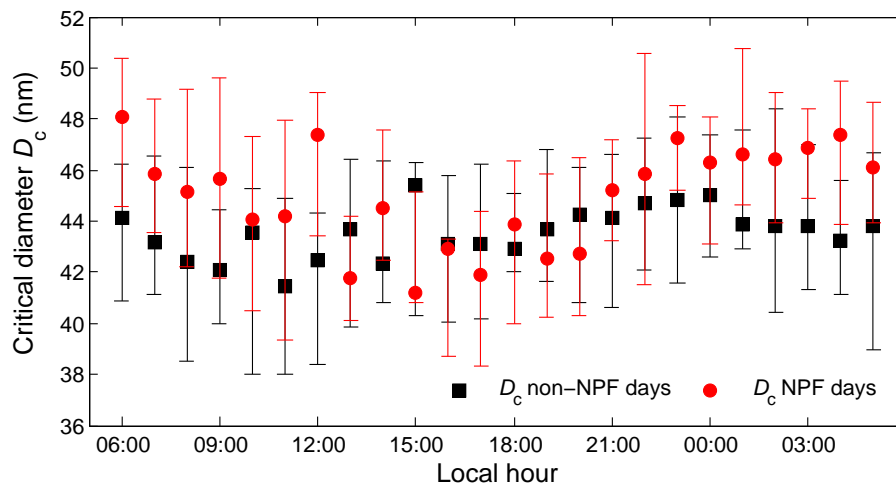
Fig. 10. Diurnal variation of median critical diameter D_c on 29 spring Type I event (red) and 53 spring non-event (black) days. Shown from 06:00 UTC + 2 of the day in question until 05:00 of the following day, for S_{eff} of 1.0 %. Error bars are 25th and 75th percentiles.

Title Page

Abstract | Introduction

Conclusions | References

Tables | Figures

|◄ | ►|

◄ | ►

Back | Close

Full Screen / Esc

Printer-friendly Version

Interactive Discussion
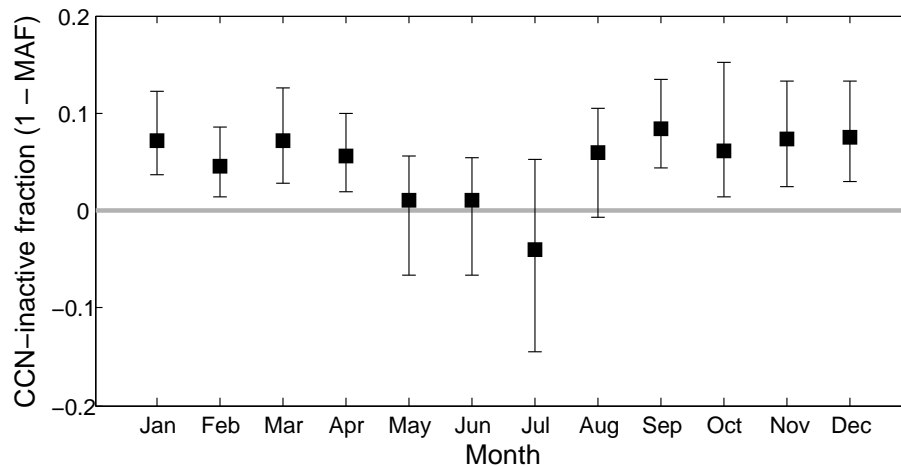
Fig. 11. Monthly median CCN-inactive fraction, calculated as 1 – MAF. Error bars are 25th and 75th percentiles.

Full Screen / Esc

Printer-friendly Version

Interactive Discussion